(12) INTERNATIONAL APPLICATION PUBLISHED UNDER THE PATENT COOPERATION TREATY (PCT)

(19) World Intellectual Property Organization
International Bureau

(43) International Publication Date
13 November 2008 (13.11.2008)

PCT

(10) International Publication Number
WO 2008/137733 A2

(51) International Patent Classification: Not classified

(21) International Application Number:
PCT/US2008/062489

(22) International Filing Date: 2 May 2008 (02.05.2008)

(25) Filing Language: English

(26) Publication Language: English

(30) Priority Data:
60/927,181 2 May 2007 (02.05.2007) US

(71) Applicant *(for all designated States except US)*: **EMORY UNIVERSITY** [US/US]; Office Of Technology Transfer, Suite 130, 1784 North Decatur Road, Atlanta, GA 30322 (US).

(72) Inventors; and

(75) Inventors/Applicants *(for US only)*: **RHYNER, Matthew, N.** [US/US]; 1510 High Haven Court, Ne, Atlanta, GA 30329 (US). **SMITH, Andrew** [US/US]; 2212 St. Clair Drive, Atlanta, GA 30329 (US). **NIE, Shuming** [US/US]; 1021 Wescott Lane, Atlanta, GA 30319 (US).

(74) Agent: **LINDER, Christopher, B.**; Thomas, Kayden, Horstemeyer & Risley, LLP., 600 Galleria Parkway, Suite 1500, Atlanta, GA 30339-5948 (US).

(81) Designated States *(unless otherwise indicated, for every kind of national protection available)*: AE, AG, AL, AM, AO, AT, AU, AZ, BA, BB, BG, BH, BR, BW, BY, BZ, CA, CH, CN, CO, CR, CU, CZ, DE, DK, DM, DO, DZ, EC, EE, EG, ES, FI, GB, GD, GE, GH, GM, GT, HN, HR, HU, ID, IL, IN, IS, JP, KE, KG, KM, KN, KP, KR, KZ, LA, LC, LK, LR, LS, LT, LU, LY, MA, MD, ME, MG, MK, MN, MW, MX, MY, MZ, NA, NG, NI, NO, NZ, OM, PG, PH, PL, PT, RO, RS, RU, SC, SD, SE, SG, SK, SL, SM, SV, SY, TJ, TM, TN, TR, TT, TZ, UA, UG, US, UZ, VC, VN, ZA, ZM, ZW.

(84) Designated States *(unless otherwise indicated, for every kind of regional protection available)*: ARIPO (BW, GH, GM, KE, LS, MW, MZ, NA, SD, SL, SZ, TZ, UG, ZM, ZW), Eurasian (AM, AZ, BY, KG, KZ, MD, RU, TJ, TM), European (AT, BE, BG, CH, CY, CZ, DE, DK, EE, ES, FI, FR, GB, GR, HR, HU, IE, IS, IT, LT, LU, LV, MC, MT, NL, NO, PL, PT, RO, SE, SI, SK, TR), OAPI (BF, BJ, CF, CG, CI, CM, GA, GN, GQ, GW, ML, MR, NE, SN, TD, TG).

Published:

— *without international search report and to be republished upon receipt of that report*

WO 2008/137733 A2

(54) **Title:** MICELLAR STRUCTURES, METHODS OF MAKING MICELLAR STRUCTURES, METHODS OF IMAGING, AND METHODS OF DELIVERING AGENTS

(57) **Abstract:** Micellar structures, methods of making micellar structures, methods of imaging (e.g., imaging cancer and diseases and their related biological systems (e.g., proteins, antibodies, and the like associated with the cancer or disease)), methods of delivering therapeutic agents and/or biological compounds, and the like, are provided.

MICELLAR STRUCTURES, METHODS OF MAKING MICELLAR STRUCTURES, METHODS OF IMAGING, AND METHODS OF DELIVERING AGENTS

CROSS-REFERENCE TO RELATED APPLICATION

This application claims priority to U.S. provisional application entitled, "MICELLAR STRUCTURES, METHODS OF MAKING MICELLAR STRUCTURES, METHODS OF IMAGING, AND METHODS OF DELIVERING AGENTS," having serial number 60/927,181, filed on May 2, 2007, which is entirely incorporated herein by reference.

STATEMENT REGARDING FEDERALLY SPONSORED RESEARCH OR DEVELOPMENT

This invention was made with government support under Grant No.: GM072069 awarded by the NIH. The government has certain rights in the invention.

BACKGROUND

The synthesis of high quality, monodisperse crystalline nanomaterials such as quantum dots (QDs) and magnetic nanoparticles (MNPs) in organic solutions has reached near perfection over the past two decades. With many of the basic chemical questions answered, attention has turned to finding significant applications for these materials. The most promising applications lie in the fields of biomedical science and clinical technology. The dramatic growth of these fields in recent years has highlighted the need for superior technologies for detection, treatment, and analysis. Systems that incorporate unique nanomaterials and are specially designed for biological applications will provide new, powerful tools to medical researchers. Design inspiration for such systems can be culled from the field of polymeric drug delivery, which focuses on improving the therapeutic index of anticancer compounds. Specifically, polymeric micelles formed from biocompatible amphiphilic diblock copolymers have been developed to entrap and deliver hydrophobic chemotherapeutic agents such as Taxol. These micellar systems rely

on entropic forces in aqueous solution to drive self-assembly of polymer chains around a hydrophobic core of drugs.

Realizing the qualitative similarities between hydrophobic drugs and hydrophobic nanoparticles, investigators have used similar strategies to entrap multiple nanoparticles on the interior of amphiphilic polymer micelles. In addition to the interesting physical mechanisms of this encapsulation procedure, the approach has several practical advantages for biomedical applications. One such advantage is the capability of combining multiple types of nanoparticles into a single probe to create multimodality probes that can include different imaging and therapeutic properties. Another advantage is enhancing probe signal strength through clustering of multiple nanoparticles in a small container, such that each target bound by a probe would have several reporter tags in one area as opposed to a one nanoparticle per target ligand, as in the traditional case. Further, by clustering nanoparticles in a larger construct, renal filtration can be avoided while still not encountering a threat from the reticuloendothelial system.

Previous attempts have utilized Fe_2O_3 MNPs, gold nanoparticles, carbon nanotubes, and even QDs. In each of these cases, the hydrophilic portion of the block copolymer consisted of polyacrylic acid, which has advantages in terms of facile functionalization owing to free carboxylic acid groups on the surface of these micelles, but must be crosslinked to ensure probe stability in stringent biological and chemical conditions. Another disadvantage is that carboxy functional groups on the surface of nanoparticle probes have been shown to contribute to nonspecific uptake by immune cells and protein opsonization, reducing their utility as biomedical imaging probes (Sathe, Rhyner, Nie, unpublished data). In addition, the QD-based micelles produced in these cases had very low quantum yields (maximum 5%). Further, despite using magnetic nanomaterials and QDs, no direct assessment of either MRI contrast capabilities or fluorescent imaging in relevant biological systems has been made. Finally, while each of these investigations have demonstrated small-scale synthesis of micellar probes, much larger quantities must be produced and purified before animal studies can be conducted and clinical applications envisioned.

SUMMARY

Embodiments of the present disclosure provide for micellar structures, methods of making micellar structures, methods of imaging (*e.g.*, imaging cancer and diseases and their related biological systems (*e.g.*, proteins, antibodies, and the like associated with the cancer or disease)), methods of delivering therapeutic agents and/or biological compounds, and the like.

One exemplary micellar structure, among others, includes: a plurality of nanoparticles and amphiphilic copolymers, wherein the amphiphilic copolymers include hydrophobic blocks and hydrophilic blocks, wherein the hydrophilic blocks of the amphiphilic copolymers form an outer shell around the plurality of nanoparticles, wherein the hydrophobic blocks of the amphiphilic copolymers interact with the nanoparticles within the outer shell of the micellar structure, and wherein the micellar structure is about 10 to 100 nm in diameter.

One exemplary method of making micellar structures, among others, includes: providing a nanoparticle and an amphiphilic copolymer; mixing the nanoparticle and the amphiphilic copolymer in a solvent; replacing the solvent with water; and forming the micellar structures.

One exemplary method of imaging a host, among others, includes: providing a micellar structure; administering the micellar structure to the host; and imaging the host.

These embodiments, uses of these embodiments, and other uses, features and advantages of the present disclosure, will become more apparent to those of ordinary skill in the relevant art when the following detailed description of the preferred embodiments is read in conjunction with the appended figures.

BRIEF DESCRIPTION OF THE DRAWINGS

Many aspects of the disclosure can be better understood with reference to the following drawings. The components in the drawings are not necessarily to scale, emphasis instead being placed upon clearly illustrating the principles of the present disclosure. Moreover, in the drawings, like reference numerals designate corresponding parts throughout the several views.

Fig. 1-1(A) shows a standard, empty micelle formed from block copolymers. Figs. 1-1(B) and 1-1(C) are schematic representations of the micelle design. In Fig. 1-1(A) is a schematic that illustrates that a high polymer concentration leads to singly encapsulated QDs, while Fig. 1-1(B) is a schematic that illustrates that a lower concentration leads to multiple QDs in a single micelle. The polymer shell thickness is roughly the same in both instances, but forms a much larger percentage of the total micelle diameter in configuration Fig. 1-1(A). The total polymer molecular weight is 20,200 (M_n PMMA=8700, M_n PEO=11,600, whole polymer M_w/M_n=1.45). Figs 1-1(D) and 1-1(E) show two hypothetical interactions between QD surface ligands and hydrophobic polymer chains.

Figs. 1-2(A) to 1-2(D) illustrate TEM and DLS data comparing the size and structure of single and multiple dot micelles. These data show that the nanoparticle size and composition can be varied by adjusting the starting ratio of quantum dots to amphiphilic polymer. Figs. 1-2(A) and 1-2(B) illustrate DLS and TEM data for a sample with a high QD to polymer ratio. Figs. 1-2(C) and 1-2(D) illustrate the same data for a lower ratio. The data also demonstrate that at very high polymer concentrations (low QD-polymer ratios), samples tend to be more monodisperse. The scale bars are 20 nm.

Figs. 1-3(A) to 1-3(B) illustrate fluorescent images and spectral data show that the micelle encapsulated QDs are stable and bright in water (high QD-polymer ratio). Fig. 1-3(A) is a true color image (shown in black and white) taken on a epiflourescent microscope under excitation with a mercury arc lamp. The scale bar is 10 microns. Fig. 1-3(B) shows both the well-defined absorption and narrow emission spectra of these micelle encapsulated QDs.

Figs. 1-4(A) to 1-4(B) illustrate the determination of the PEO-PMMA polymer critical micelle concentration (cmc) (from top to bottom the concentrations are: 1 mg/mL, 10^{-1} mg/mL, $10^{-1.5}$ mg/mL, 10^{-2} mg/mL, $10^{-2.5}$ mg/mL, 10^{-3} mg/mL, $10^{-3.5}$ mg/mL, 10^{-4} mg/mL, and $10^{-4.5}$ mg/mL). The fluorescent spectrum of pyrene is a function of the concentration of amphiphilic polymer in solution Fig. 1-4(A). Plotting the intensity of the largest peak (372 nm) as a function of polymer concentration approximates the cmc as the first inflection point of the curve Fig 1-4(B). The cmc of the large MW PEO-PMMA used in this research is about $10^{-1.8}$ mg/ml. The minimum final concentration of

polymer after the dialysis procedure is about $10^{-0.78}$, roughly an order of magnitude larger than the critical micelle concentration.

Fig. 1-5 illustrates a wide field TEM of a sample with a high QD-polymer ratio.

Fig. 1-6 illustrates a wide field TEM of a sample with a low QD-polymer ratio.

Figs. 2-1(A) and 2-1(B) illustrate an embodiment of an illustrative approach to creation of size and composition tunable micellar probes. Fig. 2-1(A) is a schematic that illustrates that high polymer:QD ratios produce singly encapsulated nanoparticle probes. Fig. 2-1(B) is a schematic that illustrates that lower polymer:QD ratios produce multinanoparticle probes. Each sample is then passed separately through an automated high-volume chromatography system to produce our final products.

Figs. 2-2(A) to 2-2(D) are TEM and DLS data comparing the size and structure of single and multiple QD micelles. Figs. 2-2(A) and 2-2(B) illustrate DLS and TEM data for a sample with a low polymer: QD molar feeding ratio (100:1). Fig. 2-2(C) and 2(D) illustrate the same data for a higher molar ratio (500:1). The scale bars are 20 nm.

Figs. 2-3(A) to 2-3(C) illustrate fluorescent and magnetic resonance characterization data for optomagnetic probes. Fig. 2-3(A) illustrates fluorescent emission and absorption for the 1:2 MNP:QD feeding ratio micelle sample, while Fig. 2-3(B) illustrates normalized T2 relaxivity curves for each of the samples in Fig. 2-3(C). Images in Fig 2-3(C) were taken on a Philips 1.5 Tesla MRI scanner.

Figs. 2-4(A) to 2-4(D) illustrate chromatograms and TEMs of micelles separated using FPLC. Fig. 2-4(A) illustrates chromatograms of UV (pink) absorption and refractive index (blue) from a 100:1 Polymer:QD sample separated using Superose 6 packing. Figs. 2-4(B) and 2-4(C) show TEMs corresponding to the peaks in Fig. 2-4(A). It is important to note that the UV absorbance peak occurs when the bulk of micelles exit the system while the RI peak occurs when the empty polymeric micelles exit. Fig. 2-4(B) is a TEM image of the collected first peak, while Fig. 2-4(C) shows the collected second peak. Finally, Fig. 2-4(D) illustrates the UV profile for the micelles fed through a column with a larger pore-size (sephadex 500HR).

Fig. 3-1 illustrates polymers used for the two approaches in this Example 3. In approach I, we synthesized a polymer of similar size and structure to our core PMMA-PEO. In Approach II, a very different structure was used to dope our PEO shell.

Figs. 3-2(A) and 3-2(B) illustrate flourescamine assay demonstrating existence of free amines. Fig. 3-2(A) shows fluorescamine signal from deprotected (top) and protected (bottom) NH2-tba-PEO saturated in pure water while Fig. 3-2(B) shows micelles incorporating deprotected NH2-tba-PEO in increasing ratios.

Figs. 3-3(A) to 3-3(B) illustrate chromatograms of conjugated and non-conjugated micelles. Fig. 3-3(A) illustrates the difference in elution time between folic acid conjugated micelles (blue) and non-conjugated micelles (pink). Fig. 3-3(B) illustrates the entire chromatogram for the post-conjugation reaction. The extremely large UV peaks are the characteristic chromatograms for free folic acid.

Fig. 3-4 illustrates FPLC chromatograms of various polymer samples. UV-vis chromatograms obtained after eluting commercial PMMA-PEO (red), heterobifunctional PEO (light blue) and conjugated PMMA-PEO-NH2 through a sephacrose 200 column. The intensitites of absorbance are normalized.

Figs. 4-1(A) to 4-1(D) illustrate fluorescent microscopy data taken at 40x. Nanoparticles were incubated with human granulocytes (stained with FITC) in the presence of plasma for 24 hours. Fig. 4-1 (A) illustrates a field of granulocytes incubated with polyacrylic acid coated QDs. Fig. 4-1 (B) illustrates two cells from the sample in Fig. 4-1 (A). Fig. 4-1 (C) illustrates a field of granulocytes incubated QDs entrapped in PEO-PMMA micelles. Fig. 4-1 (D) illustrates two cells from sample in Fig. 4-1(C).

Figs. 4-2(A) to 4-2(D) illustrate digital flourescent micrographs comparing micelle encapsulated QDs with carboxylated QDs. Micelles (Fig. 4-2(A)(top left)) and QD-COOH (Fig. 4-2(B)(top right)) both spread uniformly on coverslips without plasma incubation. After incubation for 6 hours with plama, the micelle encapsulated QDs (Fig. 4-2(C)(bottom left)) still spread uniformly while the carobxylated QDs (Fig. 4-2(D)(bottom right)) are significantly aggregated.

Fig. 4-3 illustrates agarose gel electrophoresis of sample with and without incubation with plasma. After incubation with plasma, QD-COOH mobility is all but stopped (lanes 1+2). Micelles do not migrate without plasma because they lack charge (lane 4). However, after incubation, they do exhibit some mobility.

DETAILED DESCRIPTION

Before the present disclosure is described in greater detail, it is to be understood that this disclosure is not limited to particular embodiments described, as such may, of course, vary. It is also to be understood that the terminology used herein is for the purpose of describing particular embodiments only, and is not intended to be limiting, since the scope of the present disclosure will be limited only by the appended claims.

Where a range of values is provided, it is understood that each intervening value, to the tenth of the unit of the lower limit (unless the context clearly dictates otherwise), between the upper and lower limit of that range, and any other stated or intervening value in that stated range, is encompassed within the disclosure. The upper and lower limits of these smaller ranges may independently be included in the smaller ranges and are also encompassed within the disclosure, subject to any specifically excluded limit in the stated range. Where the stated range includes one or both of the limits, ranges excluding either or both of those included limits are also included in the disclosure.

Unless defined otherwise, all technical and scientific terms used herein have the same meaning as commonly understood by one of ordinary skill in the art to which this disclosure belongs. Although any methods and materials similar or equivalent to those described herein can also be used in the practice or testing of the present disclosure, the preferred methods and materials are now described.

All publications and patents cited in this specification are herein incorporated by reference as if each individual publication or patent were specifically and individually indicated to be incorporated by reference and are incorporated herein by reference to disclose and describe the methods and/or materials in connection with which the publications are cited. The citation of any publication is for its disclosure prior to the filing date and should not be construed as an admission that the present disclosure is not entitled to antedate such publication by virtue of prior disclosure. Further, the dates of publication provided could be different from the actual publication dates that may need to be independently confirmed.

As will be apparent to those of skill in the art upon reading this disclosure, each of the individual embodiments described and illustrated herein has discrete components and features which may be readily separated from or combined with the features of any of the

other several embodiments without departing from the scope or spirit of the present disclosure. Any recited method can be carried out in the order of events recited or in any other order that is logically possible.

Embodiments of the present disclosure will employ, unless otherwise indicated, techniques of chemistry, synthetic organic chemistry, biochemistry, biology, molecular biology, and the like, which are within the skill of the art. Such techniques are explained fully in the literature.

The following examples are put forth so as to provide those of ordinary skill in the art with a complete disclosure and description of how to perform the methods and use the compositions and compounds disclosed and claimed herein. Efforts have been made to ensure accuracy with respect to numbers (*e.g.*, amounts, temperature, *etc.*), but some errors and deviations should be accounted for. Unless indicated otherwise, parts are parts by weight, temperature is in °C, and pressure is at or near atmospheric. Standard temperature and pressure are defined as 20 °C and 1 atmosphere.

Before the embodiments of the present disclosure are described in detail, it is to be understood that, unless otherwise indicated, the present disclosure is not limited to particular materials, reagents, reaction materials, manufacturing processes, or the like, as such can vary. It is also to be understood that the terminology used herein is for purposes of describing particular embodiments only, and is not intended to be limiting. It is also possible in the present disclosure that steps can be executed in different sequence where this is logically possible.

It must be noted that, as used in the specification and the appended claims, the singular forms "a," "an," and "the" include plural referents unless the context clearly dictates otherwise. Thus, for example, reference to "a support" includes a plurality of supports. In this specification and in the claims that follow, reference will be made to a number of terms that shall be defined to have the following meanings unless a contrary intention is apparent.

DEFINITIONS

In describing and claiming the disclosed subject matter, the following terminology will be used in accordance with the definitions set forth below.

In accordance with the present disclosure there may be employed conventional molecular biology, microbiology, and recombinant DNA techniques within the skill of the art. Such techniques are explained fully in the literature. See, *e.g.*, Maniatis, Fritsch & Sambrook, "Molecular Cloning: A Laboratory Manual (1982); "DNA Cloning: A Practical Approach," Volumes I and II (D.N. Glover ed. 1985); "Oligonucleotide Synthesis" (M.J. Gait ed. 1984); "Nucleic Acid Hybridization" (B.D. Hames & S.J. Higgins eds. (1985)); "Transcription and Translation" (B.D. Hames & S.J. Higgins eds. (1984)); "Animal Cell Culture" (R.I. Freshney, ed. (1986)); "Immobilized Cells and Enzymes" (IRL Press, (1986)); B. Perbal, "A Practical Guide To Molecular Cloning" (1984), each of which is incorporated herein by reference.

The term "polypeptides" includes proteins and fragments thereof. Polypeptides are disclosed herein as amino acid residue sequences. Those sequences are written left to right in the direction from the amino to the carboxy terminus. In accordance with standard nomenclature, amino acid residue sequences are denominated by either a three letter or a single letter code as indicated as follows: Alanine (Ala, A), Arginine (Arg, R), Asparagine (Asn, N), Aspartic Acid (Asp, D), Cysteine (Cys, C), Glutamine (Gln, Q), Glutamic Acid (Glu, E), Glycine (Gly, G), Histidine (His, H), Isoleucine (Ile, I), Leucine (Leu, L), Lysine (Lys, K), Methionine (Met, M), Phenylalanine (Phe, F), Proline (Pro, P), Serine (Ser, S), Threonine (Thr, T), Tryptophan (Trp, W), Tyrosine (Tyr, Y), and Valine (Val, V).

As used herein, the term "polynucleotide" generally refers to any polyribonucleotide or polydeoxribonucleotide, which may be unmodified RNA or DNA or modified RNA or DNA. Thus, for instance, polynucleotides as used herein refers to, among others, single-and double-stranded DNA, DNA that is a mixture of single-and double-stranded regions, single- and double-stranded RNA, and RNA that is mixture of single- and double-stranded regions, hybrid molecules comprising DNA and RNA that may be single-stranded or, more typically, double-stranded or a mixture of single- and double-stranded regions. The terms "nucleic acid," "nucleic acid sequence," or "oligonucleotide" also encompasses a polynucleotide as defined above.

In addition, polynucleotide as used herein refers to triple-stranded regions comprising RNA or DNA or both RNA and DNA. The strands in such regions may be

from the same molecule or from different molecules. The regions may include all of one or more of the molecules, but more typically involve only a region of some of the molecules. One of the molecules of a triple-helical region often is an oligonucleotide.

As used herein, the term polynucleotide includes DNAs or RNAs as described above that contain one or more modified bases. Thus, DNAs or RNAs with backbones modified for stability or for other reasons are "polynucleotides" as that term is intended herein. Moreover, DNAs or RNAs comprising unusual bases, such as inosine, or modified bases, such as tritylated bases, to name just two examples, are polynucleotides as the term is used herein.

It will be appreciated that a great variety of modifications have been made to DNA and RNA that serve many useful purposes known to those of skill in the art. The term polynucleotide as it is employed herein embraces such chemically, enzymatically, or metabolically modified forms of polynucleotides, as well as the chemical forms of DNA and RNA characteristic of viruses and cells, including simple and complex cells, inter alias.

Use of the phrase "biomolecule" is intended to encompass deoxyribonucleic acid (DNA), ribonucleic acid (RNA), nucleotides, oligonucleotides, nucleosides, polynucleotides, proteins, peptides, polypeptides, selenoproteins, antibodies, antigens, protein complexes, aptamers, haptens, combinations thereof, and the like.

Use of "biological" or "biological target" is intended to encompass biomolecules (*e.g.*, deoxyribonucleic acid (DNA), ribonucleic acid (RNA), nucleotides, oligonucleotides, nucleosides, polynucleotides, proteins, peptides, polypeptides, selenoproteins, antibodies, antigens, protein complexes, aptamers, haptens, combinations thereof) and the like. In particular, biological or biological target can include, but is not limited to, naturally occurring substances such as polypeptides, polynucleotides, lipids, fatty acids, glycoproteins, carbohydrates, fatty acids, fatty esters, macromolecular polypeptide complexes, vitamins, co-factors, whole cells, eukaryotic cells, prokaryotic cells, micelles, microorganisms such as viruses, bacteria, protozoa, archaea, fungi, algae, spores, apicomplexan, trematodes, nematodes, mycoplasma, or combinations thereof. In addition, the biological target can include native intact cells, viruses, bacterium, and the like.

"Cancer", as used herein, shall be given its ordinary meaning, as a general term for diseases in which abnormal cells divide without control. Cancer cells can invade nearby tissues and can spread through the bloodstream and lymphatic system to other parts of the body.

There are several main types of cancer, for example, carcinoma is cancer that begins in the skin or in tissues that line or cover internal organs. Sarcoma is cancer that begins in bone, cartilage, fat, muscle, blood vessels, or other connective or supportive tissue. Leukemia is cancer that starts in blood-forming tissue such as the bone marrow, and causes large numbers of abnormal blood cells to be produced and enter the bloodstream. Lymphoma is cancer that begins in the cells of the immune system.

When normal cells lose their ability to behave as a specified, controlled and coordinated unit, a tumor is formed. Generally, a solid tumor is an abnormal mass of tissue that usually does not contain cysts or liquid areas (some brain tumors do have cysts and central necrotic areas filled with liquid). A single tumor may even have different populations of cells within it, with differing processes that have gone awry. Solid tumors may be benign (not cancerous), or malignant (cancerous). Different types of solid tumors are named for the type of cells that form them. Examples of solid tumors are sarcomas, carcinomas, and lymphomas. Leukemias (cancers of the blood) generally do not form solid tumors.

Representative cancers include, but are not limited to, bladder cancer, breast cancer, colorectal cancer, endometrial cancer, head & neck cancer, leukemia, lung cancer, lymphoma, melanoma, non-small-cell lung cancer, ovarian cancer, prostate cancer, testicular cancer, uterine cancer, cervical cancer, thyroid cancer, gastric cancer, brain stem glioma, cerebellar astrocytoma, cerebral astrocytoma, glioblastoma, ependymoma, Ewing's sarcoma family of tumors, germ cell tumor, extracranial cancer, Hodgkin's disease, leukemia, acute lymphoblastic leukemia, acute myeloid leukemia, liver cancer, medulloblastoma, neuroblastoma, brain tumors generally, non-Hodgkin's lymphoma, osteosarcoma, malignant fibrous histiocytoma of bone, retinoblastoma, rhabdomyosarcoma, soft tissue sarcomas generally, supratentorial primitive neuroectodermal and pineal tumors, visual pathway and hypothalamic glioma, Wilms' tumor, acute lymphocytic leukemia, adult acute myeloid leukemia, adult non-Hodgkin's lymphoma, chronic lymphocytic leukemia, chronic myeloid leukemia, esophageal cancer, hairy cell leukemia, kidney cancer, multiple myeloma, oral cancer, pancreatic cancer, primary central nervous system lymphoma, skin cancer, small-cell lung cancer, among others.

A tumor can be classified as malignant or benign. In both cases, there is an abnormal aggregation and proliferation of cells. In the case of a malignant tumor, these cells behave more aggressively, acquiring properties of increased invasiveness. Ultimately, the tumor cells may even gain the ability to break away from the microscopic environment in which they originated, spread to another area of the body (with a very different environment, not normally conducive to their growth), and continue their rapid growth and division in this new location. This is called metastasis. Once malignant cells have metastasized, achieving a cure is more difficult.

Benign tumors have less of a tendency to invade and are less likely to metastasize. Brain tumors spread extensively within the brain but do not usually metastasize outside the brain. Gliomas are very invasive inside the brain, even crossing hemispheres. They do divide in an uncontrolled manner, though. Depending on their location, they can be just as life threatening as malignant lesions. An example of this would be a benign tumor in the brain, which can grow and occupy space within the skull, leading to increased pressure on the brain.

Use of the term "affinity" can include biological interactions and/or chemical interactions. The biological interactions can include, but are not limited to, bonding or hybridization among one or more biological functional groups located on the first biomolecule or biological target and the second biomolecule or biological target. In this regard, the first (or second) biomolecule can include one or more biological functional groups that selectively interact with one or more biological functional groups of the second (or first) biomolecule. The chemical interaction can include, but is not limited to, bonding among one or more functional groups (*e.g.*, organic and/or inorganic functional groups) located on the biomolecules.

"Treating" or "treatment" of a disease (or a condition or a disorder) includes preventing the disease from occurring in an animal that may be predisposed to the disease but does not yet experience or exhibit symptoms of the disease (prophylactic treatment), inhibiting the disease (slowing or arresting its development), providing relief from the symptoms or side-effects of the disease (including palliative treatment), and relieving the disease (causing regression of the disease). With regard to cancer, these terms also mean that the life expectancy of an individual affected with a cancer will be increased or that one or more of the symptoms of the disease will be reduced.

As used herein, the term "host" or "organism" includes humans, mammals (*e.g.*, cats, dogs, horses, *etc.*), living cells, and other living organisms. A living organism can be as simple as, for example, a single eukaryotic cell or as complex as a mammal. Typical hosts to which embodiments of the present disclosure may be administered will be mammals, particularly primates, especially humans. For veterinary applications, a wide variety of subjects will be suitable, *e.g.*, livestock such as cattle, sheep, goats, cows, swine, and the like; poultry such as chickens, ducks, geese, turkeys, and the like; and domesticated animals particularly pets such as dogs and cats. For diagnostic or research applications, a wide variety of mammals will be suitable subjects, including rodents (*e.g.*, mice, rats, hamsters), rabbits, primates, and swine such as inbred pigs and the like. Additionally, for *in vitro* applications, such as *in vitro* diagnostic and research applications, body fluids and cell samples of the above subjects will be suitable for use, such as mammalian (particularly primate such as human) blood, urine, or tissue samples, or blood, urine, or tissue samples of the animals mentioned for veterinary applications. In some embodiments, a system includes a sample and a host. The term "living host" refers to host or organisms noted above that are alive and are not dead. The term "living host" refers to the entire host or organism and not just a part excised (*e.g.*, a liver or other organ) from the living host.

The term "sample" can refer to a tissue sample, cell sample, a fluid sample, and the like. The sample may be taken from a host. The tissue sample can include hair (including roots), buccal swabs, blood, saliva, semen, muscle, or from any internal organs. The fluid may be, but is not limited to, urine, blood, ascites, pleural fluid, spinal fluid, and the like. The body tissue can include, but is not limited to, skin, muscle, endometrial, uterine, and cervical tissue. In the present disclosure, the source of the sample is not critical.

The term "detectable" refers to the ability to detect a signal over the background signal.

The term "detectable signal" is a signal derived from quantum dots. The detectable signal is detectable and distinguishable from other background signals that may be generated from the host. In other words, there is a measurable and statistically significant difference (*e.g.*, a statistically significant difference is enough of a difference to distinguish among the acoustic

detectable signal and the background, such as about 0.1%, 1%, 3%, 5%, 10%, 15%, 20%, 25%, 30%, or 40% or more difference between the detectable signal and the background) between detectable signal and the background. Standards and/or calibration curves can be used to determine the relative intensity of the acoustic detectable signal and/or the background.

DISCUSSION

In accordance with the purpose(s) of the present disclosure, as embodied and broadly described herein, embodiments of the present disclosure, in one aspect, relate to micellar structures, methods of making micellar structures, methods of imaging (*e.g.*, imaging cancer and diseases and their related biological systems (*e.g.*, proteins, antibodies, and the like associated with the cancer or disease)), methods of delivering therapeutic agents and/or biological compounds, and the like.

Embodiments of the present disclosure provide micellar structures that include nanoparticles that retain a significant portion (*e.g.*, greater than about 85% of their original properties) of their properties and characteristics (*e.g.*, spectral properties, magnetic properties, or the like) that existed prior to forming the micellar structure. The outer shell of the micellar structures provides stability in a wide range of conditions (*e.g.*, acids, bases, buffers, and/or physiological conditions).

Embodiments of the micellar structures can include two or more types of nanoparticles and/or two or more nanoparticles in the same class but having different characteristics (*e.g.*, two quantum dots each having distinct spectral characteristics), thereby providing micellar structures having multimodality characteristics. In addition, the methods of the present disclosure provide the ability to controllably "tune" the characteristics of the micellar structures.

In addition, embodiments of the present disclosure provide methods of preparing the micellar structures in high yield without significant deterioration of the nanoparticles or characteristics of the nanoparticles.

Furthermore, embodiments of the present disclosure provide micellar structures that can have therapeutic agents and/or biological agents attached to the nanoparticles and/or to the surface of the micellar structures.

Embodiments of the micellar structure include a plurality of nanoparticles and amphiphilic copolymers (*e.g.*, amphiphilic block copolymers). The amphiphilic copolymers include hydrophobic blocks and hydrophilic blocks. The micellar structure includes an inner core, an intermediate region, and an outer shell. The hydrophilic blocks of the amphiphilic copolymers form an outer shell around the plurality of nanoparticles to form the outer surface of the micellar structure. The outer shell reduces or eliminates the interaction of the nanoparticles with the environment surrounding the micellar structure. In addition, therapeutic agents and/or biological compounds can be associated with the outer shell. The hydrophobic blocks of the amphiphilic copolymers interact with the nanoparticles within the outer shell of the micellar structure to form the inner core and the intermediate region. The inner core includes the nanoparticles, while the intermediate region includes the nanoparticles and the hydrophobic blocks of the amphiphilic copolymer. The micellar structure can be about 10 to 100 nm, about 10 to 75 nm, about 10 to 65 nm, about 15 to 65 nm, or about 20 to 60 nm, in diameter.

Nanoparticles

The nanoparticles can include, but are not limited to, magnetic nanoparticles, semiconductor nanoparticles, metal nanoparticles, and metal oxide nanoparticles (*e.g.*, gold, silver, copper, titanium, or oxides thereof), metalloid and metalloid oxide nanoparticles, the lanthanide series metal nanoparticles, and combinations thereof. In general, the nanoparticles can have a diameter of about 1 to 30 nm, about 1 to 20 nm, or about 1 to 10 nm. The nanoparticles can be about 50% to 99.9%, about 60% to 99.9%, or about 85% to 99.9% weight percent of the micellar structure.

In particular, semiconductor nanoparticles include semiconductor quantum dots, which are described in more detail below and in US Patent 6,468,808 and International Patent Application WO 03/003015, each of which are incorporated herein by reference. Furthermore, the magnetic nanoparticles (*e.g.*, those having magnetic properties) can include, but are not limited to, iron nanoparticles and iron composite nanoparticles. In general, the magnetic nanoparticles include iron oxide alloys with the general formula MFe_2O_4 where M is selected from Co, Ni, Mn, Mg, Fe, Pt, and the like. Preferably, the nanoparticles are semiconductor quantum dots.

Quantum dots can include, but are not limited to, luminescent semiconductor quantum dots. In general, quantum dots include a core and a cap, however, uncapped quantum dots can be used as well. The "core" is a nanometer-sized semiconductor. While any core of the IIA-VIA, IIIA-VA, or IVA-IVA, IVA-VIA semiconductors can be used in the context of the present disclosure, the core is such that, upon combination with a cap, a luminescent quantum dot results. A IIA-VIA semiconductor is a compound that contains at least one element from Group IIA and at least one element from Group VIA of the periodic table, and so on. The core can include two or more elements. In one embodiment, the core is a IIA-VIA, IIIA-VA, or IVA-IVA semiconductor that can be about 1 nm to about 40 nm, about 1 nm to 30 nm, about 1 nm to 20 nm, or about 1 nm to 10 nm in diameter. In another embodiment, the core can be a IIA-VIA semiconductor and can be about 2 nm to about 10 nm in diameter. For example, the core can be CdS, CdSe, CdTe, ZnSe, ZnS, PbS, PbSe, or an alloy.

The "cap" is a semiconductor that differs from the semiconductor of the core and binds to the core, thereby forming a surface layer on the core. The cap typically passivates the core by having a higher band gap than the core. In one embodiment, the cap can be a IIA-VIA semiconductor of high band gap. For example, the cap can be ZnS or CdS. Combinations of the core and cap can include, but are not limited to, the cap is ZnS when the core is CdSe or CdS, and the cap is CdS when the core is CdSe. Other exemplary quantum does include, but are not limited to, CdS, ZnSe, CdSe, CdTe, $CdSe_xTe_{1-x}$, InAs, InP, PbTe, PbSe, PbS, HgS, HgSe, HgTe, CdHgTe, and GaAs. The size of the cap can be about 0.1 to 10 nm, about 0.1 to 5 nm, or about 0.1 to 2 nm in diameter. Other illustrative quantum dots can include, but are not limited to, a quantum dot having an emission at about 525 nm, a quantum dot having an emission at about 585 nm, a quantum dot having an emission at about 605 nm, a quantum dot having an emission at about 655 nm, or a quantum dot having an emission at about 685 nm.

The wavelength emitted (*e.g.*, color) by the quantum dots can be selected according to the physical properties of the quantum dots, such as the size and the material of the nanocrystal. Quantum dots are known to emit light from about 300 nanometers (nm) to 2000 nm (*e.g.*, UV, near IR, and IR). The colors of the quantum dots include, but are not limited to, red, blue, green, and combinations thereof. The color or the

fluorescence emission wavelength can be tuned continuously. The wavelength band of light emitted by the quantum dot is determined by either the size of the core or the size of the core and cap, depending on the materials that make up the core and cap. The emission wavelength band can be tuned by varying the composition and the size of the QD and/or adding one or more caps around the core in the form of concentric shells.

The synthesis of quantum dots is well known and is described in U.S. Patent Nos. 5,906,670; 5,888,885; 5,229,320; 5,482,890; 6,468,808; 6,306,736; 6,225,198, *etc.*, International Patent Application WO 03/003015, (all of which are incorporated herein by reference) and in many research articles. The wavelengths emitted by quantum dots and other physical and chemical characteristics have been described in US Patent 6,468,808 and International Patent Application WO 03/003015 and will not be described in any further detail. In addition, methods of preparation of quantum dots are described in US Patent 6,468,808 and International Patent Application WO 03/003015 and will not be described any further detail.

In an embodiment, the quantum dot can be substantially coated or coated with a polymer or another compound. The polymer can include, but is not limited to, a polyamine, a capping ligand, a hydrophobic polymer layer, hydrophillic polymer layer, amphiphillic polymer layer, di- and/or tri-block copolymer layer, and combinations thereof. The coverage of the quantum dot with the polymer can be about 1 to 100%. The thickness of the polymer layer can be about 0.5 to 50 nm.

In another embodiment, the quantum dot can be capped with a capping ligand, which forms a layer on the quantum dot, and have a polymer layer disposed on the capping ligand. The capping ligand can include compounds such as, but not limited to, an $O=PR_3$ compound, an $O=PHR_2$ compound, an $O=PHR_1$ compound, a H_2NR compound, a HNR_2 compound, a NR_3 compound, a HSR compound, a SR_2 compound, and combinations thereof. "R" can be a C_1 to C_{18} hydrocarbon such as, but not limited to, linear hydrocarbons, branched hydrocarbons, cyclic hydrocarbons, substituted hydrocarbons (*e.g.*, halogenated), saturated hydrocarbons, unsaturated hydrocarbons, and combinations thereof. Preferably, the hydrocarbon is a saturated linear C_4 to C_{18} hydrocarbon, a saturated linear C_6 to C_{18} hydrocarbon, and a saturated linear C_{18} hydrocarbon. A combination of R groups can be attached to P, N, or S. In particular, the

capping ligand can be selected from, but is not limited to, tri-octylphosphine oxide, stearic acid, and octyldecyl amine, oleic acid, and derivatives thereof.

In another embodiment, the quantum dot can be overcoated with a polymer, through interactions such as, but not limited to, hydrophobic interactions, hydrophilic interactions, covalent bonding, and the like.

The thickness of each layer disposed on the quantum dot can vary significantly depending on the particular application. In general, the thickness can be about 0.5 to 20 nm, about 0.5 to 15 nm, about 0.5 to 10 nm, or about 0.5 to 5 nm.

Amphiphilic copolymers

As mentioned above, the amphiphilic copolymers include hydrophobic blocks and hydrophilic blocks. The amphiphilic copolymer includes, but is not limited to, amphiphilic block copolymers, amphiphilic random copolymers, amphiphilic alternating copolymers, amphiphilic periodic copolymers, and combinations thereof. In an embodiment, the amphiphilic copolymer is an amphiphilic block copolymer. In an embodiment, the amphiphilic block copolymer is a polymethylmethacrylate-PEG block copolymer. Additional amphiphilic copolymers are described hereinafter.

The amphiphilic random copolymer can include, but is not limited to random copolymer poly(methyl acrylate-co-acrylic acid); random copolymer poly(methyl methacrylate-co-n-butyl acrylate); random copolymer poly(methyl methacrylate-co-hydroxypropyl acrylate); random copolymer poly(styrene-co-p-carboxyl chloro styrene); random copolymer poly(styrene-co-4-hydroxystyrene); random copolymer poly(styrene-co-4-vinyl benzoic acid); random copolymer poly(styrene-co-4-vinyl pyridine); (and combinations thereof. The amphiphilic alternating copolymer can include, but is not limited to, poly(maleic anhydride-alt-1-octadecene), poly(maleic anhydride-alt-1-tetradecene), alternating copolymer poly(carbo tert.butoxy α-methyl styrene-alt-maleic anhydride) and alternating copolymer poly(carbo tert.butoxy norbornene-alt-maleic anhydride), and combinations thereof.

The block copolymer includes amphiphilic di- and or triblock copolymers. In addition, the copolymer can include hydrocarbon side chains such as, but not limited to, 1-18-carbon aliphatic side chains, 1-18-carbon alkyl side chains, and combinations

thereof. Furthermore, the di or tri block copolymers have at least one hydrophobic block and at least one hydrophilic block.

The following is an exemplary list of amphiphilic random and alternating copolymers: random copolymer poly(dimethyl siloxane-co-diphenyl siloxane); random copolymer poly(methyl acrylate-co-acrylic acid); random copolymer poly(methyl methacrylate-co-n-butyl acrylate); random copolymer poly(methyl methacrylate-co-t-butyl acrylate); random copolymer poly(methyl methacrylate-co-hydroxypropyl acrylate); random copolymer poly(tetrahydrofuranyl methacrylate-co-ethyl methacrylate); random copolymer poly(styrene-co-4-bromostyrene); random copolymer poly(styrene-co-butadiene); random copolymer poly(styrene-co-diphenyl ethylene); random copolymer poly(styrene-co-t-butyl methacrylate); random copolymer poly(styrene-co-t-butyl-4-vinyl benzoate); random copolymer poly(styrene-co-p-carboxyl chloro styrene); random copolymer poly(styrene-co-p-chloromethyl styrene); random copolymer poly(styrene-co-methyl methacrylate); random copolymer poly(styrene-co-4-hydroxystyrene); random copolymer poly(styrene-co-4-vinyl benzoic acid); random copolymer poly(styrene-co-4-vinyl pyridine); alternating copolymer poly(carbo tert.butoxy α-methyl styrene-alt-maleic anhydride); alternating copolymer poly(carbo tert.butoxy norbornene-alt-maleic anhydride); alternating copolymer poly(α-methyl styrene-alt-methyl methacrylate); and alternating copolymer poly(styrene-alt-methyl methacrylate).

The following is an exemplary list of amphiphilic copolymers: poly((meth)acrylic acid) based copolymers (*e.g.*, poly(acrylic acid-b-methyl methacrylate); poly(methyl methacrylate-b-acrylic acid); poly(methyl methacrylate-b-sodium acrylate); poly(sodium acrylate-b-methyl methacrylate); poly(methacrylic acid-b-neopentyl methacrylate); poly(neopentyl methacrylate-b-methacrylic acid); poly(t-butyl methacrylate-b-ethylene oxide); poly(methyl methacrylate-b-sodium methacrylate); and poly(methyl methacrylate-b-N,N-dimethyl acrylamide), polydiene and hydrogenated polydiene based copolymers (*e.g.*, poly(butadiene(1,2 addition)-b-methylacrylic acid; poly(butadiene(1,4 addition)-b-acrylic acid); poly(butadiene(1,4 addition)-b-sodium acrylate); poly(butadiene(1,4 addition)-b-ethylene oxide; poly(butadiene(1,2 addition)-b-ethylene oxide); poly(butadiene(1,2 addition)-b-ethylene oxide)-hydroxy benzoic ester terminal group; 4-methoxy benzyolester terminated poly(butadiene-b-ethylene oxide) diblock

copolymer; poly(butadiene-b-N-methyl 4-vinyl pyridinium iodide); poly(isoprene-b-N-methyl 2-vinyl pyridinium iodide); poly(isoprene-b-ethylene oxide) (1,4 addition); poly(isoprene-b-ethylene oxide) (1,2 and 3,4 addition); poly(propylene-ethylene-b-ethylene oxide); and hydrogonated poly(isoprene-b-ethylene oxide) (1,2 addition)), hydrogentated diene based copolymers (*e.g.*, poly(ethylene-b-ethylene oxide) and poly(isoprene-b-ethylene oxide)), poly(ethylene oxide) based copolymers (*e.g.*, poly(ethylene oxide-b-acrylic acid); poly(ethylene oxide-b-ε-caprolactone); poly(ethylene oxide-b-6-(4'-cyanobiphenyl-4-yloxy)hexyl methacrylate); poly(ethylene oxide-b-lactide); poly(ethylene oxide-b-2-hydroxyethyl methacrylate); poly(ethylene oxide-b-methyl methacrylate); poly(-methyl methacrylate-b- ethylene oxide); poly(ethylene oxide-b-methacrylic acid); poly(ethylene oxide-b-2-methyl oxazoline); poly(ethylene oxide-b-propylene oxide); poly(ethylene oxide-b-t-butyl acrylate); poly(ethylene oxide-b-tetrahydrofurfuryl methacrylate); and poly(ethylene oxide-b-N,N-dimethylethylmethacrylate)), polyisobutylene based copolymers (*e.g.*, poly(isobutylene-b-ethylene oxide)), polystyrene based copolymers (*e.g.*, poly(styrene-b-acrylic acid); poly(styrene-b-sodium acrylate); poly(styrene-b-acrylamide); poly(p-chloromethyl styrene-b-acrylamide); poly(styrene-co-p-chloromethyl styrene-b-acrylamide); poly(styrene-co-p-chloromethyl styrene-b-acrylic acid); poly(styrene-b-cesium acrylate); poly(styrene-b-ethylene oxide); poly(4-styrenesulfonic acid-b-ethylene oxide); poly(styrene-b-methacrylic acid); poly(styrene-b-sodium methacrylate); poly(styrene-b-N-methyl 2-vinyl pyridinium iodide); and poly(styrene-b-N-methyl-4-vinyl pyridinium iodide)), polysiloxane based copolymers (*e.g.*, poly(dimethylsiloxane-b-acrylic acid)), poly(2-vinyl naphthalene) based copolymers (*e.g.*, poly(2-vinyl naphthalene-b-acrylic acid)), poly (vinyl pyridine and N-methyl vinyl pyridinium iodide) based copolymers (*e.g.*, poly(2-vinyl pyridine-b-ethylene oxide); poly(N-methyl 2-vinyl pyridinium iodide-b-ethylene oxide); and poly(N-methyl 4-vinyl pyridinium iodide-b-methyl methacrylate)).

The following in an exemplary list of amphiphilic diblock copolymers: poly(meth)acrylate based copolymers (*e.g.*, poly(n-butyl acrylate-b-methyl methacrylate); poly(n-butyl acrylate-b-dimethylsiloxane-co-diphenyl siloxane); poly(t-butyl acrylate-b-methyl methacrylate); poly(t-butyl acrylate-b-4-vinylpyridine); poly(2-ethyl hexyl

acrylate-b-4-vinyl pyridine); poly(t-butyl methacrylate-b-2-vinyl pyridine); poly(2-hydroxyl ethyl acrylate-b-neopentyl acrylate); poly(2-hydroxyl ethyl methacrylate-b-neopentyl methacrylate); poly(2-hydroxyl ethyl methacrylate-b-n-butyl methacrylate); poly(2-hydroxyl ethyl methacrylate-b-t-butyl methacrylate); poly(methyl methacrylate-b-acrylonitrile); poly(methyl methacrylate-b-t-butyl methacrylate); poly(isotactic methyl methacrylate-b-syndiotactic methyl methacrylate); poly(methyl methacrylate-b-t-butyl acrylate); poly(methyl methacrylate-b-trifluroethyl methacrylate); poly(methyl methacrylate-b-2-hydroxyethyl methacrylate with cholesteryl chloroformate); poly(methyl methacrylate-b-disperse red 1 acrylate); poly(methyl methacrylate-b-2-hydroxyethyl methacrylate); poly(methyl methacrylate-b-neopentyl acrylate); and poly(methacrylate-b-2-pyranoxy ethyl methacrylate)), polydiene based copolymers (*e.g.*, poly(butadiene(1,2 addition)-b-i-butyl methacrylate); poly(butadiene(1,2 addition)-b-s-butyl methacrylate); poly(butadiene(1,4 addition)-b-t-butyl acrylate; poly(butadiene(1,2 addition)-b-t-butyl acrylate; poly(butadiene(1,2 addition)-b-t-butyl methacrylate); poly(butadiene(1,4 addition)-b-ε-caprolactone); poly(butadiene((1,4 addition)-b-dimethylsiloxane); poly(butadiene(1,4 addition)-b-methyl methacrylate) (syndiotactic); poly(butadiene(1,2 addition)-b-methyl methacrylate); poly(butadiene(1,4 addition)-b-4-vinyl pyridine; poly(isoprene(1,4 addition)-b-methyl methacrylate(syndiotactic)); poly(isoprene(1,4 addition)-b-2-vinyl pyridine; poly(isoprene(1,2 addition)-b-4-vinyl pyridine); and poly(isoprene(1,4 addition)-b-4-vinyl pyridine)), polyisobutylene based copolymers (*e.g.*, poly(isobutylene-b-t-butyl methacrylate); poly(isobutylene-b-ε-caprolactone); poly(isobutylene-b-dimethylsiloxane); poly(isobutylene-b-methyl methacrylate); poly(isobutylene-b-4-vinyl pyridine), polystyrene based copolymers (*e.g.*, poly(styrene-b-n-butyl acrylate); poly(styrene-b-t-butyl acrylate); poly(styrene-b-t-butyl acrylate), broad distribution; poly(styrene-b-disperse red 1 acrylate); poly(p-chloromethyl styrene-b-t-butyl acrylate); poly(styrene-b-N-isopropyl acrylamide); poly(styrene-b-n-butyl methacrylate); poly(styrene-b-t-butyl methacrylate); poly(styrene-b-cyclohexyl methacrylate); poly(styrene-b-2-cholesteryloxycarbonyloxy ethyl methacrylate); poly(styrene-b-N,N-dimethyl amino ethyl methacrylate); poly(styrene-b-ethyl methacrylate); poly(styrene-b-2-hydroxyethyl methacrylate); poly(styrene-b-2-hydroxypropyl methacrylate); poly(styrene-b-methyl methacrylate); poly(styrene-b-

methylmethacrylate); poly(styrene-b-n-propyl methacrylate); poly(styrene-b-butadiene(1,4 addition)); poly(styrene-b-butadiene(1,2 addition)); poly(styrene-b-isoprene(1,4 addition)); poly(styrene-b-isoprene(1,2 addition or 3,4 addition)); poly(styrene-b-isoprene(1,4 addition)), hydrogenated; tapered block copolymer poly(styrene-b-butadiene); tapered block copolymer poly(styrene-b-ethylene); poly(styrene-b-ε-caprolactone); poly(styrene-b-l-lactide); poly(styrene-b-dimethylsiloxane), trimethylsilane endgroup; poly(styrene-b-dimethylsiloxane), silanol endgroup; poly(styrene-b-methyl phenyl siloxane); poly(styrene-b-ferrocenyldimethylsilane); poly(styrene-b-t-butyl styrene); poly(styrene-b-t-butoxystyrene); poly(styrene-b-4-hydroxyl styrene); poly(4- amino benzyl-b-styrene); poly(styrene-b-2-vinyl pyridine); poly(styrene-b-4-vinyl pyridine); and poly(α-methylstyrene-b-4-vinyl pyridine), poly(vinyl naphthalene) based copolymers (*e.g.*, poly(2-vinyl naphthalene-b- n-butyl acrylate), poly(2-vinyl naphthalene-b- t-butyl acrylate); poly(2-vinyl naphthalene-b- methyl methacrylate); and poly(2-vinyl naphthalene-b- dimethylsiloxane)), poly(vinyl pyridine) based copolymers (*e.g.*, poly(2-vinyl pyridine-b-ε-caprolactone); poly(2-vinyl pyridine-b-methyl methacrylate); and poly(4-vinyl pyridine-b-methyl methacrylate)), poly (propylene oxide-b-ε-caprolactone) (*e.g.*, poly (propylene oxide-b-ε-caprolactone)), polysiloxane based copolymers (*e.g.*, poly(dimethylsiloxane-b-n-butyl acrylate); poly(dimethylsiloxane-b-t-butyl acrylate); poly(dimethylsiloxane-b-t-butyl methacrylate); poly(dimethylsiloxane-b-ε-caprolactone); poly(dimethylsiloxane-b-6-(4'-cyanobiphenyl-4-yloxy)hexyl methacrylate); poly(dimethylsiloxane-b-1-ethoxy ethyl methacrylate); poly(dimethylsiloxane-b-hydroxy ethyl acrylate); and poly(dimethylsiloxane-b-methyl methacrylate)), adipic anhydride based copolymers (*e.g.*, poly(ethylene oxide-b-adipic anhydride); poly(propylene oxide-b-adipic anhydride); poly(dimethyl siloxane-b-adipic anhydride); poly(methyl methacrylate-b-adipic anhydride); and poly(2-vinyl pyridine-b-adipic anhydride)).

The following in an exemplary list of amphiphilic a-b-a triblock copolymers: poly((meth)acrylate) based triblock copolymers (*e.g.*, poly(n-butyl acrylate-b-9,9-di-n-hexyl-2,7-fluorene -b-n-butyl acrylate); poly(t-butyl acrylate-b-9,9-di-n-hexyl-2,7-fluorene -b-t-butyl acrylate); poly(acrylic acid-b-9,9-di-n-hexyl-2,7-fluorene -b- acrylic acid); poly(t-butyl acrylate-b-methyl methacrylate-b-t-butyl acrylate); poly(t-butyl

acrylate-b-styrene-b-t-butyl acrylate); poly(methyl methacrylate-b-butadiene(1,4 addition)-b-methyl methacrylate); poly(methyl methacrylate-b-n-butyl acrylate-b-methyl methacrylate); poly(methyl methacrylate-b-t-butyl acrylate-b-methyl methacrylate); poly(methyl methacrylate-b- t-butyl methacrylate acid-b-methyl methacrylate); poly(methyl methacrylate-b-methacrylic acid-b-methyl methacrylate); poly(methyl methacrylate-b-dimethylsiloxane-b-methyl methacrylate); poly(methyl methacrylate-b-9,9-di-n-hexyl-2,7-fluorene -b-methyl methacrylate); poly(methyl methacrylate-b-styrene-b-methyl methacrylate); poly(trimethylamonium iodide ethyl methacrylate-b-9,9-di-n-hexyl-2,7-fluorene-b- trimethylamonium iodide ethyl methacrylate); poly(N,N-dimethyl amino ethyl methacrylate-b-9,9-di-n-hexyl-2,7-fluorene-b-N,N-dimethyl amino ethyl methacrylate); and poly(N,N-dimethyl amino ethyl methacrylate-b-propylene oxide-b-N,N-dimethyl amino ethyl methacrylate)), polybutadiene based triblock copolymers (*e.g.*, poly(butadiene(1,4 addition)-b-styrene-b-butadiene(1,4 addition))), poly(oxirane) based triblock copolymers (*e.g.*, poly(ethylene oxide-b-9,9-di-n-hexyl-2,7-fluorene -b-ethylene oxide); poly(ethylene oxide-b-propylene oxide-b-ethylene oxide); poly(ethylene oxide-b-styrene-b-ethylene oxide); and poly(propylene oxide-b-dimethyl siloxane-b-propylene oxide)), polylactone and polylactide diblock copolymers (*e.g.*, poly(lactide-b-ethylene oxide-b-lactide); poly(caprolactone-b-ethylene oxide-b-caprolactone); and alpha,-ω diacrylonyl terminated poly(lactide-b-ethylene oxide-b-lactide)), polyoxazoline based triblock copolymers (*e.g.*, poly(2-methyl oxazoline-b-dimethyl siloxane-b-2-methyl oxazoline))), polystyrene based triblock copolymers (*e.g.*, poly(styrene-b-acrylic acid-b-styrene); poly(styrene-b-butadiene (1,4 addition) -b-styrene); poly(styrene-b-butadiene (1,2 addition) -b-styrene); poly(styrene-b-butylene-b-styrene); poly(styrene-b-n-butyl acrylate-b-styrene); poly(styrene-b-t-butyl acrylate-b-styrene); poly(styrene-b-9,9-di-n-hexyl-2,7-fluorene-b-styrene); poly(styrene-b-ethyl acrylate-b-styrene); poly(styrene-b-isoprene-b-styrene); poly(styrene-b-ethylene oxide-b-styrene); poly(styrene-b-4-vinyl pyridine-b-styrene); and poly(styrene-b-dimethyl siloxane-b-styrene)), poly(vinyl pyridine) based triblock copolymers (*e.g.*, poly(2-vinyl pyridine-b-butadiene(1,2 addition)-b-2-vinyl pyridine); poly(2-vinyl pyridine-b-styrene-b-2-vinyl pyridine); and poly(4-vinyl pyridine-b-styrene-b-4-vinyl pyridine).

The following in an exemplary list of amphiphilic a-b-c triblock copolymers: poly(styrene-b-butadiene-b-methyl methacrylate) (*e.g.*, poly(styrene-b-butadiene-b-methyl methacrylate)), poly(styrene-b-butadiene-b-2-vinyl pyridine) (*e.g.*, poly(styrene-b-butadiene-b-2-vinyl pyridine)), poly(styrene-b-t-butyl acrylate-b-methyl methacrylate) (*e.g.*, poly(styrene-b-t-butyl acrylate-b-methyl methacrylate)), poly(styrene-b-isoprene-b-glycidyl methacrylate) (*e.g.*, poly(styrene-b-isoprene-b-glycidyl methacrylate)), poly(styrene-b-2-vinyl pyridine-b-ethylene oxide) (*e.g.*, poly(styrene-b-2-vinyl pyridine-b-ethylene oxide)), poly(styrene-b-anthracene methyl methacrylate-b-methymethacrylate) (*e.g.*, poly(styrene-b-anthracene methyl methacrylate-b-methymethacrylate)), poly(styrene-b-t-butyl acrylate-b-2-vinyl pyridine) (*e.g.*, poly(styrene-b-t-butyl acrylate-b-2-vinyl pyridine)), and poly(styrene-b-t-butyl methacrylate-b-2-vinyl pyridine) (*e.g.*, poly(styrene-b-t-butyl methacrylate-b-2-vinyl pyridine)).

The following in an exemplary list of amphiphilic funtionalized diblock and triblock copolymers: amino terminated poly(dimethylsiloxane-b-diphenylsiloxane); amino terminated poly(styrene-b-isoprene); amino terminated poly(ethylene oxide-b-lactone); hydroxy terminated poly(styrene-b-2-vinyl pyridine); hydroxy terminated polystyrene-b-poly(methyl methacrylate); α-hydroxy terminated poly(styrene-b-butadiene(1,2-addition)); 4-methoxy benzyolester terminated poly(butadiene-b-ethylene oxide) diblock copolymer; succinic acid terminated poly(butadiene-b-ethylene oxide) diblock copolymer; α,ω-disuccinimidyl succinate terminated poly(ethylene oxide-propylene oxide-ethylene oxide); cabinol at the junction of poly(styrene-b-isoprene(1,4 addition)); and silane at the junction of poly(styrene-b-2-vinyl pyridine).

In addition, the following is an exemplary list of amphiphilic block copolymers: poly(1-vinylpyrrolidone-co-vinyl acetate); poly(ethylene-co-propylene-co-5-methylene-2-norbornene); poly(styrene-co-acrylonitrile); poly(2-vinylpyridine-*co*-styrene); poly(ethylene-co-methacrylic acid) sodium salt; poly(acrylonitrile-co-butadiene-co-styrene); poly(vinyl chloride-co-vinyl acetate-co-maleic acid); poly(ethylene-co-vinyl acetate); poly(ethylene-co-ethyl acrylate); poly(4-vinylpyridine-*co*-styrene); poly(vinyl butyral-*co*-vinyl alcohol-*co*-vinyl acetate); poly(methyl methacrylate co-methacrylic acid); poly-(vinyl chloride-co-vinyl acetate-co-hydroxypropyl acrylate); Luviquat®HM 552; poly(vinyl chloride-co-vinyl acetate-co-vinyl alcohol); poly(styrene-co-

divinylbenzene); poly(DL-lactide-*co*-glycolide); poly(acrylonitrile-co-methyl acrylate); poly[(vinyl chloride-*co*-(1-methyl-4-vinylpiperazine)]; poly(2-isopropenyl-2-oxazoline-*co*-methyl methacrylate); poly(tetrafluoroethylene oxide-co-difluoromethylene oxide) α,ω-diol, ethoxylated; poly[dimethylsiloxane-*co*-methyl(3-hydroxypropyl)siloxane]-*graft*-poly(ethylene glycol) methyl ether; poly(acrylonitrile-co-methacrylonitrile); poly(ethylene-co-1-butene); poly(vinylidene fluoride co-hexafluoropropylene); poly(ethylene-co-1-octene); poly(ethylene-co-methyl acrylate); poly(acrylonitrile-co-butadiene), amine terminated; poly(perfluoropropylene oxide-*co*-perfluoroformaldehyde); poly(butyl methacrylate-*co*-isobutyl methacrylate); poly(styrene-co-maleic anhydride), partial isooctyl ester, cumene terminated; poly(acrylonitrile-*co*-butadiene-*co*-acrylic acid), dicarboxy terminated; poly(vinyl alcohol-*co*-ethylene); poly(dimethylsiloxane-co-methylphenylsiloxane); poly(styrene-co-maleic anhydride); poly(Bisphenol A-co-epichlorohydrin); poly(styrene-co-butadiene); poly[(R)-3-hydroxybutyric acid-co-(*R*)-3-hydroxyvaleric acid]; poly(vinyl alcohol-*co*-vinyl acetate-co-itaconic acid); poly(methylstyrene-co-indene), hydrogenated; poly(4-vinylphenol-*co*-2-hydroxyethyl methacrylate); poly(styrene-co-maleic anhydride), cumene terminated; poly(methyl methacrylate-*co*-ethylene glycol dimethacrylate); poly(ethylene-co-propylene); poly(styrene-co-maleic acid), partial isobutyl/methyl mixed ester; poly(Bisphenol A-co-epichlorohydrin), glycidyl end-capped; poly(methyl methacrylate-*co*-methacrylic acid); poly(2-acrylamido-2-methyl-1-propanesulfonic acid-*co*-acrylonitrile); poly(propylene-co-tetrafluoroethylene); poly(butyl methacrylate-*co*-methyl methacrylate); poly(dimethylsiloxane-co-alkylmethylsiloxane); poly(acrylic acid-*co*-acrylamide) potassium salt; poly(oxymethylene-co-1,3-dioxepane); poly(chlorotrifluoroethylene-co-vinylidene fluoride); poly(melamine-co-formaldehyde), acrylated solution; poly(pentafluorostyrene-*co*-glycidyl methacrylate); poly(1,1,1,3,3,3-hexafluoroisopropyl methacrylate-*co*-glycidyl methacrylate); poly(2,2,3,4,4,4,-hexafluorobutyl methacrylate-*co*-glycidyl methacrylate); poly(2,2,3,3,3-pentafluoropropyl methacrylate-*co*-glycidyl methacrylate); poly[(propylmethacryl-heptaisobutyl-PSS)-*co*-(*n*-butylmethacrylate)]; poly(pyromellitic dianhydride-*co*-4,4'-oxydianiline), amic acid solution; poly(*tert*-butyl methacrylate-*co*-glycidyl methacrylate); poly[(propylmethacryl-heptaisobutyl-PSS)-*co*-hydroxyethylmethacrylate]; poly[(*m*-

phenylenevinylene)-*co*-(2,5-dioctoxy-*p*-phenylenevinylene)]; poly[(methylmethacrylate)-*co*-(9-anthracenylmethyl methacrylate)]; poly[(methylmethacrylate)-*co*-(2-naphthylacrylate)]; poly[methylmethacrylate-*co*-(7-(4-trifluoromethyl)coumarin methacrylamide)]; poly[(methylmethacrylate)-*co*-(9-anthracenylmethyl acrylate)]; poly[(methylmethacrylate)-*co*-(9*H*-carbazole-9-ethylmethacrylate)]; poly[(propylmethacryl-heptaisobutyl-PSS)-*co*-(methylmethacrylate)]; poly[(isobutylene-*alt*-maleic acid), ammonium salt)-*co*-(isobutylene-*alt*-maleic anhydride)]; poly(ethylenecarbonyl-co-propylenecarbonyl); poly[4,5-difluoro-2,2-bis(trifluoromethyl)-1,3-dioxole-*co*-tetrafluoroethylene]; poly(dimethylsiloxane-*co*-diphenylsiloxane), trimethylsilyl terminated; poly(dimethylsiloxane-*co*-methylhydrosiloxane), trimethylsilyl terminated; poly(dimethylsiloxane-*co*-diphenylsiloxane), divinyl terminated; poly(styrene-*co*-methyl methacrylate); poly(styrene-co-α-methylstyrene); poly(1,4-cyclohexanedimethylene terephthalate-*co*-ethylene terephthalate); Amberjet™ 4200; poly[dimethylsiloxane-*co*-methyl(3-hydroxypropyl)siloxane]-*graft*-poly(ethylene glycol) [3-(trimethylammonio)propyl chloride] ether solution; poly[dimethylsiloxane-*co*-methyl(3-hydroxypropyl)siloxane]-*graft*-poly(ethylene/propylene glycol); poly(ethylene-co-butyl acrylate); poly(ethylene-co-ethyl acrylate-co-maleic anhydride); poly(ethyl methacrylate-*co*-methyl acrylate); poly(ethylene-co-1-butene-co-1-hexene); poly(melamine-co-formaldehyde), isobutylated solution; poly[Bisphenol A carbonate-co-4,4'-(3,3,5-trimethylcyclohexylidene) diphenol carbonate]; poly(acrylamide-*co*-acrylic acid); poly(styrene-co-maleic acid), partial sec-butyl/methyl mixed ester; poly(4-hydroxybenzoic acid-co-6-hydroxy-2-naphthoic acid); poly[butylene terephthalate-co-poly(alkylene glycol) terephthalate]; poly(ethylene-*co*-vinyl acetate-*co*-methacrylic acid); poly(melamine-co-formaldehyde), methylated; poly(acrylonitrile-co-butadiene), dicarboxy terminated; poly(vinyl chloride-co-vinyl acetate-co-2-hydroxypropyl acrylate); poly(tetrafluoroethylene oxide-co-difluoromethylene oxide) α,ω-diol; poly(melamine-co-formaldehyde), butylated solution; poly[(phenyl glycidyl ether)-co-formaldehyde]; poly(acrylamide-*co*-diallyldimethylammonium chloride) solution; poly(tetrafluoroethylene-co-perfluoro(propylvinyl ether)); poly(4-vinylpyridine-*co*-butyl methacrylate); poly(dimer acid-co-alkyl polyamine); poly(1-vinylpyrrolidone-*co*-2-dimethylaminoethyl

methacrylate), quaternized solution; poly(methyl methacrylate-*co*-ethyl acrylate); Luviquat®FC 550; poly(vinyltoluene-co-α-methylstyrene); poly(epichlorohydrin-co-ethylene oxide-co-allyl glycidyl ether); poly(dimethylsiloxane-*co*-methylhydrosiloxane); polybutadiene-graft-poly(methyl acrylate-co-acrylonitrile); poly(styrene-co-maleic anhydride), partial 2-butoxyethyl ester, cumene terminated; poly(dimethylamine-co-epichlorohydrin) solution; poly(ethylene-*co*-acrylic acid); poly(acrylamide-*co*-acrylic acid) partial sodium salt; poly(hexafluoropropylene oxide-co-difluoromethylene oxide) monoalkylamide; poly(1-vinylpyrrolidone-*co*-2-dimethylaminoethyl methacrylate) solution; poly(acrylic acid-*co*-maleic acid) sodium salt; poly(ethylene-*co*-acrylic acid, zinc salt); poly(ethylene-co-tetrafluoroethylene); poly(2,2,2-trifluoroethyl methacrylate-*co*-glycidyl methacrylate); poly(pentabromophenyl acrylate-*co*-glycidyl methacrylate); poly(2,2,3,3,4,4,4-heptafluorobutyl methacrylate-*co*-glycidyl methacrylate; poly[methylmethacrylate-*co*-(disperse yellow 7 methacrylate)]; poly(2,2,3,3-tetrafluoropropyl methacrylate-*co*-glycidyl methacrylate); poly(pentabromophenyl methacrylate-*co*-glycidylmethacrylate); poly[methylmethacrylate-*co*-(Disperse Orange 3 methacrylamide)]; poly[((*S*)-()-1-(4-nitrophenyl)-2-pyrrolidinemethyl)acrylate-*co*-methylmethacrylate]; poly[(methylmethacrylate)-*co*-(Disperse Red 13 methacrylate)]; poly[(methylmethacrylate)-*co*-(Disperse Red 13 acrylate)]; poly[methylmethacrylate-*co*-(*N*-(1-naphthyl)-*N*-phenylacrylamide)]; poly[(propylmethacryl-heptaisobutyl-PSS)-*co*-styrene]; poly(pyromellitic dianhydride-*co*-thionin); poly(ethylene glycol)-*co*-4-benzyloxybenzyl alcohol, polymer-bound; poly[(isobutylene-*alt*-maleimide)-*co*-(isobutylene-*alt*-maleic anhydride)]; poly[dimethylsiloxane-*co*-(3-aminopropyl)methylsiloxane]; poly[dimethylsiloxane-*co*-[3-(2-(2-hydroxyethoxy)ethoxy)propyl)methylsiloxane]; poly(vinylidene chloride-*co*-acrylonitrile-*co*-methyl methacrylate); poly(ethylene-co-1,2-butylene)diol; poly(DL-lactide-*co*-caprolactone) (40:60); poly(methyl methacrylate-*co*-butyl methacrylate); poly(tetrafluoroethylene oxide-co-difluoromethylene oxide)α,ω-diol bis(2,3-dihydroxypropyl ether); poly[dimethylsiloxane-*co*-(2-(3,4-epoxycyclohexyl)ethyl)methylsiloxane]; poly(vinyl chloride-co-isobutyl vinyl ether); poly(indene-co-coumarone); poly(styrene-co-4-bromostyrene-co-divinylbenzene); poly(ethylene-*co*-butyl acrylate-*co*-carbon monoxide); poly(vinyl acetate-co-butyl

maleate-co-isobornyl acrylate) solution; poly(3,3',4,4'-benzophenonetetracarboxylic dianhydride-co-4,4'-oxydianiline/1,3-phenylenediamine), amic acid (solution); poly(tetrafluoroethylene-co-vinylidene fluoride-co-propylene); poly(ethylene-co-methacrylic acid) lithium salt; poly(styrene-*co*-butadiene-*co*-methyl methacrylate); poly(vinylidene chloride-co-vinyl chloride); poly(styrene-co-maleic acid), partial isobutyl ester; poly[4,4'-methylenebis(phenyl isocyanate)-alt-1,4-butanediol/poly(ethylene glycol-co-propylene glycol/polycaprolactone]; poly(ethylene-co-methacrylic acid); poly(isobutylene-*co*-maleic acid) sodium salt; poly(ethylene-co-methacrylic acid) zinc salt; poly(4-styrenesulfonic acid-*co*-maleic acid) sodium salt; poly(acrylonitrile-*co*-butadiene-*co*-acrylic acid), glycidyl methacrylate diester; poly(urea-co-formaldehyde), butylated solution; poly(ethylene-*co*-methyl acrylate-*co*-glycidyl methacrylate); poly[(phenyl glycidyl ether)-co-dicyclopentadiene]; poly[(o-cresyl glycidyl ether)-co-formaldehyde]; poly(urea-co-formaldehyde), methylated; poly(acrylic acid-*co*-maleic acid) solution; poly(3-hydroxybutyric acid-*co*-3-hydroxyvaleric acid); poly(p-toluenesulfonamide-co-formaldehyde); poly(styrene-co-allyl alcohol); poly(2-acrylamido-2-methyl-1-propanesulfonic acid-*co*-styrene); poly(acrylonitrile-co-butadiene); poly(4-vinylphenol-*co*-methyl methacrylate); poly[dimethylsiloxane-*co*-methyl(3-hydroxypropyl)siloxane]-*graft*-poly(ethylene-*ran*-propylene glycol) methyl ether; poly(hexafluoropropylene oxide-co-difluoromethylene oxide) monoamidosilane; poly(dimethylamine-co-epichlorohydrin-co-ethylenediamine) solution; poly(ethylene-*co*-butyl acrylate-*co*-maleic anhydride); poly(trimellitic anhydride chloride-*co*-4,4'-methylenedianiline); poly[methylmethacrylate-*co*-(Disperse Orange 3 acrylamide)]; poly[((*S*)-()-1-(4-Nitrophenyl)-2-pyrrolidinemethyl)methacrylate-*co*-methylmethacrylate]; poly[(propylmethacryl-heptaisobutyl-PSS)-*co*-(*t*-butylmethacrylate)]; poly[(methylmethacrylate)-*co*-(2-naphthylmethacrylate)]; poly[methylmethacrylate-*co*-(fluorescein*O*-acrylate)]; poly[methylmethacrylate-*co*-(fluorescein*O*-methacrylate)]; poly{[2-[2',5'-bis(2''-ethylhexyloxy)phenyl]-1,4-phenylenevinylene]-*co*-[2-methoxy-5-(2'-ethylhexyloxy)-1,4-phenylenevinylene]}; poly[(methylmethacrylate)-*co*-(Disperse Red 1 acrylate)]; poly(4-hydroxy benzoic acid-*co*-ethylene terephthalate); poly(vinylidene chloride-co-acrylonitrile); poly(dimethylsiloxane-*co*-diphenylsiloxane), dihydroxy terminated; poly(1,4-butylene

adipate-*co*-1,4-butylene succinate), extended with 1,6-diisocyanatohexane; poly(dicyclopentadiene-co-*p*-cresol); poly[ethyl acrylate-co-methacrylic acid-co-3-(1-isocyanato-1-methylethyl)-α-methylstyrene], adduct with ethoxylated nonylphenol solution; poly(epichlorohydrin-co-ethylene oxide); poly(Bisphenol A-co-4-nitrophthalic anhydride-co-1,3-phenylenediamine); poly(ethylene-*co*-methyl acrylate-*co*-acrylic acid); poly(propylene-co-1-butene); Nylon 6/66; poly(ethylene-*co*-acrylic acid) sodium salt; poly(ethylene-*co*-vinyl acetate-*co*-carbon monoxide); poly(melamine-co-formaldehyde), methylated/butylated (55/45); poly(maleic acid-co-olefin) sodium salt solution; poly(tetrafluoroethylene oxide-co-difluoromethylene oxide) α,ω-diisocyanate; poly(lauryl methacrylate-*co*-ethylene glycol dimethacrylate); poly[(phenyl isocyanate)-co-formaldehyde]; poly[2,6-bis(hydroxymethyl)-4-methylphenol-co-4-hydroxybenzoic acid]; poly(tetrafluoroethylene oxide-co-difluoromethylene oxide) α,ω-dicarboxylic acid; poly[methylmethacrylate-*co*-(Disperse yellow 7 acrylate)]; poly[(methylmethacrylate)-*co*-(9*H*-carbazole-9-ethylacrylate)]; poly[methylmethacrylate-*co*-(*N*-(1-naphthyl)-*N*-phenylmethacrylamide)]; poly[(methylmethacrylate)-*co*-(Disperse Red 1 methacrylate)]; poly(L-lactide-*co*-caprolactone-*co*-glycolide); poly[methylmethacrylate-*co*-(7-(4-trifluoromethyl)coumarin acrylamide)]; poly[dimethylsiloxane-*co*-methyl(3,3,3-trifluoropropyl)siloxane]; poly[dimethylsiloxane-*co*-methyl(stearoyloxyalkyl)siloxane]; poly(hexafluoropropylene oxide-co-difluoromethylene oxide) alcohol, ethoxylated phosphate; poly(ethylene-co-1,2-butylene) mono-ol; poly[dimethylsiloxane-*co*-methyl(3-hydroxypropyl)siloxane]-*graft*-tetrakis(1,2-butylene glycol); poly(1,4-butylene adipate-*co*-polycaprolactam); poly(vinyl acetate-co-crotonic acid); poly(tert-butyl acrylate-co-ethyl acrylate-co-methacrylic acid); poly(1-vinylpyrrolidone-co-styrene); poly(tetrafluoroethylene oxide-co-difluoromethylene oxide)-α,ω-bis(methyl carboxylate); poly(vinylidene chloride-co-methyl acrylate); poly(acrylonitrile-*co*-vinylidene chloride-*co*-methyl methacrylate); poly(styrene-co-maleic anhydride), partial cyclohexyl/isopropyl ester, cumene terminated; poly(4-ethylstyrene-co-divinylbenzene); poly(dimethylsiloxane-*co*-dimer acid), bis(perfluorododecyl) terminated; poly(styrene-co-maleic anhydride), partial propyl ester, cumene terminated; poly(dimer acid-co-ethylene glycol), hydrogenated; poly(ethylene-*co*-glycidyl methacrylate); poly[dimethylsiloxane-*co*-methyl(3-hydroxypropyl)siloxane]-*graft*-poly(ethylene glycol)

3-aminopropyl ether; poly(dimer acid-co-1,6-hexanediol-co-adipic acid), hydrogenated; poly(3,3',4,4'-biphenyltetracarboxylic dianhydride-co-1,4-phenylenediamine), and amic acid solution; and poly[*N,N'*-bis(2,2,6,6-tetramethyl-4-piperidinyl)-1,6-hexanediamine-co-2,4-dichloro-6-morpholino-1,3,5-triazine].

In addition, the block copolymer can be used with, or in some embodiments replaced with, a detergent and/or a lipid. For example, the detergents can include, but are not limited to, AOT, brij family, lgepal family, triton family, SDS, and derivatives of each. In particular, the detergents can include, dioctyl sulfosuccinate sodium salt, polyethylene glycol dodecyl ether, octylphenoxy polyethoxyethanol, octylphenyl-polyethylene glycol, t-octylphenoxypolyethoxyethanol, polyethylene glycol tert-octylphenyl ether, 4-(1,1,3,3-tetramethylbutyl)phenyl-polyethylene glycol, dodecyl sulfate sodium salt, and glycolic acid ethoxylate octyl ether. Further, the block copolymer can include lipids such as, but not limited to, lipid-PEG, natural lipids, synthetic lipids, sphingolipids, and derivatives of each.

The amphiphilic copolymer can be about 0.1% to 20%, about 0.1% to 10%, or about 0.1% to 5% weight of the micellar structure.

Therapeutic agents, biological compounds (*e.g.*, a protein, an antibody, a polynucleotide, a polypeptide, and an aptamer), linkers, and/or other compounds can be attached directly to the outer shell of the amphiphilic copolymer. The therapeutic agent and/or the biological compound can be attached through functional groups and/or linkers to the outer shell of amphiphilic copolymer. In an embodiment, the therapeutic agent and/or biological compound can be attached in series via one or more linkers. The functional group can include, but is not limited to, SH, OH, COOH, NH_3, and the like, as well as combinations thereof. In an embodiment, the functional group is part of the hydrophilic blocks of the amphiphilic copolymer. During the preparation of the micellar structure, the functional group can be protected. In other words, an end-protected amphiphilic copolymer (*e.g.*, tBMA-PEO-functional group-protecting group) can be used with the amphiphilic copolymer. Appropriate protecting groups for the selected amphiphilic copolymer are known in the art. The micellar structure surface will include the end-protected amphiphilic copolymer and the amphiphilic copolymer. Once the micellar structure is prepared, the protecting group can be removed from the end-

protected amphiphilic copolymer. Subsequently the micellar structure can be introduced to a therapeutic agent, a biological compound, and/or a linker that can react with the unprotected functional group. The amount of the end-protected amphiphilic copolymer can be about 0.0001 to 50 % of the copolymer solution.

The therapeutic agents, the biological compounds, the linkers, and/or other compounds, can be linked to the outer shell of amphiphilic copolymer using any stable physical and/or chemical association to the outer shell of amphiphilic copolymer directly or indirectly by any suitable means. For example, the component can be linked to the outer shell of amphiphilic copolymer using a covalent link, a non-covalent link, an ionic link, and a chelated link, as well as being absorbed or adsorbed onto the outer shell of amphiphilic copolymer. In addition, the component can be linked to the outer shell of amphiphilic copolymer through hydrophobic interactions, hydrophilic interactions, charge-charge interactions, π-stacking interactions, combinations thereof, and like interactions.

The linker can include a functional group (*e.g.*, an amine group) on the outer shell of amphiphilic copolymer and/or the linker can include a separate compound attached to the outer shell of amphiphilic copolymer or the layer at one end and the protein, the antibody, the polynucleotide, the polypeptide, the aptamer, the linker, other compounds, or another linker at the other end. The linker can include functional groups such as, but not limited to, amines, carboxylic acids, hydroxyls, thios, and combinations thereof. The linker can include compounds such as, but not limited to, diethylene triamine pentaacetic acid (DTPA), ethylene diamine tetraacetic acid (EDTA), 3,4-dihydroxyphenylalanine (DOPA), ethylene glycol tetraacetic acid (EGTA), nitrilo triacetic acid (NTA), and combinations thereof. In an embodiment, the linker and the chelator compound are the same, but in other embodiments they can be different. The percentage of linkers attached to the chelator compound, contrast agent, and/or another linker can be about 0.1 to about 100%.

Methods of making micellar structures

Embodiments of the present disclosure include methods of making micellar structures. The methods apply towards any one or a combination of the nanoparticles

and/or any one or more of the amphiphilic copolymers. For reasons of clarity, an exemplary embodiment of the method will be described in reference to a single type of nanoparticle and a single type of amphiphilic copolymer. However, the methods of the present disclosure can be applied to micellar structures including more than one type or class of nanoparticle and/or more than one type or class of amphiphilic copolymer.

Initially, the nanoparticle and the amphiphilic copolymer are prepared. In an embodiment of the nanoparticle, a stabilizing ligand is used in the preparation of the nanoparticle. The selection of the stabilizing ligand should consider the interaction of the stabilizing ligand with the amphiphilic copolymer. For example, trioctylphosphine oxide is compatible with the amphiphilic copolymer (*e.g.*, polymethylmethacrylate-PEG block copolymer) used in an embodiment of the present disclosure so it can be used as the stabilizing ligand for the preparation of the quantum dots.

The selection of the amphiphilic copolymer should include the following considerations: polymer molecular weight, polymer composition (*e.g.*, ratio of hydrophobic to hydrophilic groups), the molecular structure of each block (*e.g.*, the hydrophobic block should form strong bonds (covalent) with the ligand on the nanoparticle), the compatibility of the amphiphilic copolymer with the nanoparticle and any ligands disposed on the nanoparticle, the purity of the amphiphilic copolymer, and the like. In an embodiment, the amphiphilic copolymer can be biocompatible and/or biodegradable. In an embodiment, the amphiphilic copolymer once incorporated into the micellar structure should show stability towards acids, bases, and/or buffers, as well as in physiological conditions.

In an embodiment, a small percentage of an end-protected amphiphilic block copolymer can be included in the copolymer solution with the amphiphilic block copolymer. The end-protected amphiphilic block copolymer and the amphiphilic block copolymer are mixed in the appropriate ratios prior to assembly of the micellar structure via dialysis. After dialysis, the protection group can be removed through standard chemistry, thus freeing the amine group for reaction with biomolecule agents, linkers, and/or therapeutic agents.

Subsequently, the purified nanoparticle and the amphiphilic copolymer are mixed in an appropriate solvent system. In one embodiment, the entire procedure is carried out

in an inert atmosphere, which helps to retain nanoparticles properties. The solvents should include the following characteristics: miscible in water, solubilize the nanoparticles, and solubilize the amphiphilic copolymers. An exemplary solvent can be tetrahydrofuran (THF). In addition the solvent can include mixtures of solvents. Exemplary solvents include, but are not limited to, methanol, isopropyl alcohol, ethanol, 1,4 dioxane, dimethyl sulfoxide, n,n-dimethlyformamide, acetnonitrile, acetone and combinations thereof. The ratio of nanoparticle to amphiphilic copolymer is about 1 to 100, about 1 to 50, or about 1 to 5. The ratio of the nanoparticle and the amphiphilic copolymer can be used to determine the final size and composition of the micelles. For example, for a multi-nanoparticle micelle, the polymer to nanoparticles ration may be 10 moles polymer: 1 mole nanoparticles.

After mixing the nanoparticle and the amphiphilic copolymer in the solvent, the solvent must be removed and replaced with water. The water should totally replace the solvent, leaving only residual amounts (<0.001% by volume). An exemplary method of replacing the solvent with water includes dialysis. The solvent mixture is used in dialysis against ultrapure water (20 M ohms resistivity) with a dialysis membrane of a low molecular weight cutoff. In one embodiment, the molecular weight cut-off of the nitroceulluose dialysis bag is approximately 2000 Daltons, but the procedure can be performed with any type of dialysis bag with a molecular weight all the way up to the weight of the polymer being used. For example, if the polymer's total molecular weight is 10,000, the dialysis bag cut off could be up to 9,999 Daltons. It may even be possible for the dialysis bag to have a molecular weight cutoff that is above the molecular weight of the polymer, since polymer chains are in a hydrated, folded state that could give them a larger apparent (hydrodynamic) molecular weight. The procedure can be carried out at room temperature, but also down to 1° C or up to 90° C. In general, the dialysis procedure takes approximately 12 hours and has multiple changes of the water (to provide fresh ultrapure water).

Using a dialysis method is advantageous compared to traditional methods (*e.g.*, sonication, solvent evaporation, step-wise addition, evaporation-re-suspension, dropwise addition and the like) because the traditional methods provide a low yield, cause aggregation, and can damage the nanoparticle. In particular, sonication can oxidize

quantum dot surfaces and eliminate fluorescence, while dropwise addition has low yield (a small amount of nanoparticles are encapsulated while the majority is precipitated), causes aggregation, and incompletely removes solvent. In contrast, the dialysis method is gentle, meaning it protects the inherent nanoparticles properties, provides high yields (about 50 to 90 % encapsulation), easy to use, and reproducible (batch-to-batch variability in size distribution and fluorescent and magnetic properties is low). In addition, the dialysis drives the formation of the micellar structure. Although not intending to be bound by theory, the osmotic pressure slowly forces the water into the dialysis bag and the extremely hydrophobic nanoparticles begin to cluster together to reduce their exposure to the aqueous environment. The clustering is then stabilized by the assembly of the amphiphilic polymers around the nanoparticles to form the micellar structures. This is an entropically driven process, as the water is seeking to minimize its interaction with the extremely hydrophobic nanoparticles. As such, micelle properties can be tuned by altering the polymer properties such as molecular weight, composition, relative percentage hydrophobic:hydrophilic content.

Once the solvent is replaced with water, the excess of amphiphilic copolymer is removed. An exemplary method for removing the excess amphiphilic copolymer includes multiple rounds of ultracentrifugation and/or centrifugation. The ultracentrifugation spins down the micellar structures while leaving the amphiphilic copolymer in solution. Any aggregation can be removed by low-speed centrifugation. A typical ultracentrifugation round is carried out for about 1 hour at 500,000 gs and a typical centrifugation is about 20 minutes at 6000 gs. Both are carried out at room temperature. Any other unit operations familiar to chemists, biochemists, and biologists can be used to remove the excess amphiphilic copolymer, and these include, but are not limited to, secondary dialysis with a larger pore bag, gel-permeation chromatography, HPLC, and the like.

Methods of use

As mentioned above, the present disclosure relates generally to methods for detecting, localizing, and/or quantifying biological targets, cellular events, diagnostics, cancer and disease imaging, gene expression, protein studies and interactions, and the

like. The present disclosure also relates to methods for multiplex imaging inside a host living cell, tissue, or organ, or a host living organism, using embodiments of the present disclosure. The present disclosure also relates to diagnosing the presence of diseases and cancer, treating diseases and cancer, monitoring the progress of diseases and cancer, and the like.

The biological target can include, but is not limited to, viruses, bacteria, cells, tissue, the vascular system, microorganisms, artificially constituted nanostructures (*e.g.*, micelles), proteins, polypeptides, antibodies, antigens, aptamers (polypeptide and polynucleotide), haptens, polynucleotides, and the like, as well as those biological targets described in the definition section above.

The methods for imaging and treating cancer include, but are not limited to, methods of imaging precancerous tissue, cancer, and tumors; methods of treating precancerous tissue, cancer, and tumors; methods of diagnosing precancerous tissue, cancer, and tumors; methods of monitoring the progress of precancerous tissue, cancer, and tumors; and the like.

In short, the micellar structure is introduced to the host living cell, tissue, or organ, or a host living organism using known techniques. The micellar structure can also be labeled with one or more types of agents and/or compounds for the particular study, as mentioned above. In particular, the micellar structure may include an agent or compound having an affinity for a biological target (*e.g.*, cancer, disease, cell types, proteins, antibodies, and the like) of interest. In addition, a single agent can be associated with two or more types of micellar structures, where the micellar structure includes nanoparticles with different characteristics (*e.g.*, spectral qualities and/or detection qualities (*e.g.*, multi-modality detection)).

Subsequently, the host living cell, tissue, or organ, or the host living organism is exposed to an appropriate excitation and/or detection source that is capable of causing the nanoparticles (*e.g.*, quantum dot) of the micellar structure to emit an energy that can be detected. In another embodiment, the host living cell, tissue, or organ, or the host living organism is exposed to an appropriate detection source that can detect the nanoparticles (*e.g.*, magnetic and/or nuclear) present in the micellar structure.

Once the micellar structure is detected, the information derived from the detection can be used to localize and/or quantify one or more features of the system being studied. For example, the micellar structure can include a biological compound having an affinity for a biological target (*e.g.*, another biological compound; cell; cancer; a tumor; a precancerous cell; biological compounds associated with a disease, a tumor, a precancerous cell; and the like). Thus, the imaging of the micellar structure can be used to determine the presence of the biological target. In another embodiment, the micellar structure can include a therapeutic agent and/or a biological compound, where the imaging of the micellar structure can be used to determine where the micellar structure was delivered (*e.g.*, to the target of interest).

In another embodiment, the micellar structure can include a biological compound having an affinity for a biological target and a therapeutic agent and/or a biological compound. Thus, the imaging can be used to determine if the micellar structure was delivered to the biological target of interest (delivery of the therapeutic agent and/or a biological compound to the biological target).

In another embodiment, the imaging of the micellar structure can be used to determine the state of the disease, cancer, a tumor, a precancerous cell, and the like over a period of time. In this embodiment, the micellar structure is administered to the host living cell, tissue, or organ, or the host living organism over a period of time (*e.g.*, days, weeks, months, and years).

Kits

This disclosure encompasses kits, which include, but are not limited to, micellar structure and directions (written instructions for their use). The components listed above can be tailored to the particular study to be undertaken. The kit can further include appropriate buffers and reagents known in the art for administering various combinations of the components listed above to the host cell or host organism.

In addition, this disclosure encompasses kits, which include, but are not limited to, components to make the micellar structures and directions for making the micellar structures. The components and directions are described in detail in above and in the Examples.

Examples 1 to 4

Now having described the embodiments of the present disclosure, in general, examples 1 to 4 describe some additional embodiments of the present disclosure. While embodiments of the present disclosure are described in connection with examples 1 to 4 and the corresponding text and figures, there is no intent to limit embodiments of the present disclosure to these descriptions. On the contrary, the intent is to cover all alternatives, modifications, and equivalents included within the spirit and scope of embodiments of the present disclosure.

Example 1

We have encapsulated hydrophobic quantum dots (QDs) in biocompatible polymeric micelles while retaining their brightness and photostability. In the last few years, researchers have focused great attention on applying QDs to biological systems. The first step in application development is to produce water soluble QDs with surface coatings useful for biological studies while retaining QDs unique optical properties. Using design principles from the field of drug delivery, we have selected biocompatible amphiphilic di-block copolymers with large polyethylene oxide (PEO) hydrophilic segments to self-assemble QDs on the interior of micelles. The unique assembly and separations procedures can be used to precisely control the number of nanocrystals on the interior of each micelle and obtain uniform size distributions. This new design, combined with a high level of control over the final size and composition of the micelles will open new avenues of investigation for the field of drug delivery and for basic quantum dot phenomena.

We have approached the issue with the intent to develop useful delivery systems for targeting cancers with novel nanoscale imaging agents. Fig. 1-1 shows that we added thick polyethylene oxide chains to reduce opsonization by the reticuloendothelial system in vivo, used FDA approved polymers to make the micelles as biocompatible as possible, and ensured preservation of the high quality and brightness of the QDs used. Fig. 1-1 also shows the micelles' tertiary structure. The inner core contains either single QDs or multiple QDs and their capping ligands. The middle band may contain some quantum dots embedded in a hydrophobic polymer layer, or solely hydrophobic polymer,

depending on the number of quantum dots encapsulated. The outer band of the micelles contains no quantum dots, and is composed of a very large chain PEO segment (264 repeat units).

Fig. 1-2 shows TEM and dynamic light scattering (DLS) data verifying that we have produced dot loaded micelles with uniform size distributions. In Figs. 1-2(A) and 1-2(B), the starting ratio of quantum dots to amphiphiles is approximately five times the case in Figs. 1-2(C) and 1-2(D). This larger ratio of dots to polymers causes multiple QDs to cluster together on the interior of the polymeric micelles. The TEM images in conjunction with DLS data imply that single-dot micelles have an average diameter of 11.0 nm and the multiple QD micelles shown in Fig. 1-1(C) have an average diameter of 31.9 nm. However, the size distribution of multiple dot micelles can be easily modified by adjusting the pre-assembly ratio of quantum dot concentration to polymer concentration. In general, it is better to use a larger initial QD concentration than a lower polymer concentration because polymer concentrations which are too low can lead to uncontrollable aggregation of the nanocrystals. Higher polymer concentrations also lead to more monodisperse micelle systems, as can be seen by comparing Figs. 1-2(A) and 1-2(C).

The control of size distribution and number of QDs per micelles makes the dot loaded micelles ideal for passively targeting cancer in mice. The enhanced permeability and retention (EPR) effect causes nanoparticles and macromolecules which are under 200 nm in size to be preferentially trapped inside tumors. Tuning the size of these biocompatible micelles will allow investigators to systematically study how size affects targeting through the EPR effect. In addition, we have also shown that the same polymers can be used to encapsulate multiple QD colors and magnetic nanoparticles (unpublished data), which will allow the biocompatible polymer micelle to serve as a delivery vehicle for a host of high quality, hydrophobic nanomaterials.

Fig. 1-3 shows that the dots spectral properties are well conserved throughout the encapsulation process. The dots emit at 632 nm with very narrow peaks (FWHM = 20) both prior to and proceeding encapsulation. Quantum yield measurements indicate that the dots retain about 85% of their pre-encapsulated quantum yield. Interestingly, when excited under a fluorescent microscope, blinking is observed both in the case of the

multiple dot and single dot micelles. As expected, there is a reduction in the degree of blinking for multiple dot micelles, but it is not eliminated. This suggests that the assembly of dots into polymeric micelles may be used as a platform to study blinking behavior, which is poorly understood. For instance, these observations imply a minimum number of QDs in a certain area causes blinking to cease. By carefully controlling the number of dots encapsulated in each micelle, investigators could determine this dot-per-area limit.

Fig. 1-4 shows the micelle concentration of the amphiphilic block copolymer. We determined that throughout the encapsulation process, our polymers are at a concentration at least an order of magnitude larger than the critical micelle concentration. This supports the inference that the process is a driven by self-assembly and demonstrates control and understanding of the system.

Fig. 1-5 is a wide field TEM image of purified, multiple-nanoparticle micelle. This image demonstrates our ability to create large populations of these micelles, and is in good agreement with the other data presented here. Fig. 1-6 is a similar image of singly encapsulated nanoparticles. These images visually demonstrate our ability to produce pure, uniform, stable micelles at desired sizes.

We have created exceptionally bright micelles through a combination of novel QD synthesis and washing procedures (not published) and judicious polymer choice. The best micelle structures are produced using a polymethylmethacrylate (PMMA)-polyethylene oxide (PEO) block copolymer. Both polymers are FDA approved for *in vivo* use, PMMA being a commonly used orthopedic cement, and PEO a commonplace coating for device implants. The QDs are core-shell dots with a thin ZnS shell coating a CdSe core. The dots are stabilized with octadecylamine capping ligands. In the assembly procedure, the QDs are precipitated from their excess capping ligands and re-suspended in tetrahydrofuran (THF) at a desired concentration. The PEO-PMMA polymers are weighed and suspended in THF. The two solutions are then centrifuged and filtered to remove any contaminants and mixed together in a dialysis bag with a low molecular weight cutoff (2000 MW). Dialysis against nanopure water is allowed to continue overnight, with several changes of the water solution. The resulting solution is

then subjected to several rounds of centrifugation, ultracentrifugation, and concentration until a highly monodisperse, concentrated solution is obtained.

In summary, we have presented a unique system incorporating QDs on the interior of biocompatible block copolymer micelles. The micelles are unique in their ability to control the number of nanocrystals on the interior, to provide a large MW PEO coating, and to protect the optical properties of the QDs. This technology is versatile, and can be used for researching tumor targeting and the basic physical properties of QDs such as blinking.

Example 2

This Example presents a novel and robust imaging platform incorporating quantum dots and magnetic nanoparticles on the interior of biocompatible micelles formed from amphiphilic block copolymers. In this Example, we describe a unique synthesis that is facile and highly scalable. The synthetic approach relies on spontaneous self-assembly of amphiphilic polymers and nanoparticles. Extensive physical characterization by dynamic light scattering and TEM shows excellent control over size and composition of these probes. Magnetic resonance and spectral characterization demonstrate enhanced biomedical imaging capabilities owing to the high quality of the starting nanomaterials. By simply adjusting the volumes and concentrations of starting materials, we can tune the probe size from those containing single nanoparticles (mean diameter = 11 nm) to large-multinanoparticle systems (mean diameter 31 nm). In addition, the same strategy can be used to tailor magnetic and fluorescent properties to those demanded by end-use applications. Further, we demonstrate that our polyethylene oxide coated probes are stable after 24 hours of incubation at 37^0C in fresh human plasma. Finally, we show that these micellar probes exhibit dramatic reduction in uptake by immune cells as opposed to other similar encapsulation strategies utilizing polyacrylic acid based block copolymers. The synthetic approach and resulting probes presented here demonstrate high potential for multimodal in vivo imaging.

In this Example, we used the same principles to form clusters of nanomaterials on the interior of amphiphilic block copolymer micelles using the procedure described in Fig. 2-1. However, we used MNPs and QDs synthesized via high-temperature organic

solvent synthesis, and block copolymers containing polyethylene oxide (PEO) as the hydrophilic block. Further, we describe a new purification approach that allows scale up to volumes necessary for detailed animal studies. Thus, the synthetic approach and micelles produced here have the following advantages: (1) they are formed from biocompatible polymers with a PEO surface optimal for biological applications, which we qualitatively demonstrate is more suitable for biological assays than polyacrylic acid based coatings (2) using high-quantum yield QD starting materials coated in octadecyl amine produces stable, bright probes with a maximum quantum yield of 40%, 8x brighter than the maximum attainable with other QDs (3) we use a previously published high-temperature organic solvent synthesis procedure to produce Fe_3O_4 MNPs, which may exhibit stronger T2-weighted MRI imaging capabilities, as opposed to the Fe_2O_3 MNPs used previously, (4) by using fast protein liquid chromatography (FPLC) to purify our multicomponent micelles, we increase yields and quantities produced dramatically, as opposed to centrifugation methods describe previously, and (5) the probes demonstrate remarkable stability in corrosive biological and chemical conditions, even without crosslinking.

As shown in Fig. 2-3, we were able to tune the T2 relaxivity of dual modality optomagnetic probes while retaining the exceptional optical properties of QDs by varying the relative ratios of QDs to MNPs in our dialysis feeding ratio. Figure 2-3(A) shows that even after incorporation of MNPs, the optical properties of QDs are well conserved. As expected, there is some observed loss in QD fluorescence as compared to QD-only micelle probes, which increases with the MNP loading ratio. This loss has been noted previously and is most likely due to the broad optical absorption spectra of mixed valence Fe_3O_4 MNPs. This highlights another advantage of the approach used here: previous attempts to create dual modality micellar probes have focused on use of γ - Fe_2O_3 MNPs, while we have used Fe_3O_4. Since the saturation magnetization of pure Fe_3O_4 is greater than that of γ - Fe_2O_3 (NAT biotech, 2001, 19, p. 1141, which is incorporated herein by reference for the corresponding discussion) we can use smaller amounts of iron oxide nanoparticles to achieve the same level of T2 contrast. As a result, for biomedical imaging application, moderate MNP:QD ratios would suffice, thus maximizing both the MRI contrast capabilities and optical brightness of these probes.

Figs. 2-4(A), 2-4(B), and 2-4(C) demonstrate the capability of FPLC to efficiently and rapidly separate nanoparticle loaded micelles from the surrounding excess polymer using Superose 6 packing. Fig. 2-4(A) shows the UV-absorbance profile in pink and the refractive index profile in blue. It is important to note that the UV absorbance peak occurs when the bulk of micelles exit the system while the RI peak occurs when the empty polymeric micelles exit, as should be expected. Fig. 2-4(B) is a digital TEM image of the collected first peak, while Fig. 2-4(C) shows the collected second peak. Finally, Fig. 2-4(D) shows the chromatogram for the micelles fed through a column with a larger pore-size and bed volume column packing (Sephadex 500HR), demonstrating that very fine gradients (represented by fractions 1, 2, and 3) can be collected.

FPLC has several advantages as compared to ultracentrifugation. First, there is no appreciable aggregation caused by the technique, meaning the final yields are much higher than with centrifugation. Secondly, by choosing different column pore size and elution volumes, fine gradients can be collected and scale up is easy to achieve. Thirdly, by automating the system, operator error is all but eliminated ensuring consistent, reproducible results. Finally, the process takes much less time and effort than running multiple 1.5 hour rounds of ultracentrifugation and centrifugation. The dialysis procedure can easily produce greater than 10 mL of unpurified nanoparticle-loaded micelles with a final concentration of roughly 5 mg/mL. After multiple rounds of centrifugation and ultracentrifugation, however, it is not uncommon to only produce 500 μL of pure samples at 2-3 mg/mL. The new FPLC approach can easily produce 10-15 mL of purified product at similar concentrations, and has the added advantage of being able to separate micelles containing many nanoparticles from those containing only a few.

MATERIALS

Octadecene (ODE; 90%) and Octadecylamine (ODA; 99%), Atto-610, Resolve-AI, and all solvents were purchased from Sigma Aldrich. Poly(methyl methacrylate)-polyethylene oxide(PMMA-PEO) diblock copolymer (PMMA-PEO; 20,300 KDa; 43% PMMA, 57% PEO) was obtained from Polymer Source. Healthy donor blood was obtained through standard venipuncture technique using 20-gauge needle (BD Medical,

Franklin Lakes) and 10 mL CellSave vacutainer collection tubes (Immunicon Inc., Huntington Valley, PA) containing anti-coagulant disodium EDTA. Blood samples were stored at room temperature until use. It should be noted that all experiments were performed on fresh blood (no longer than 2 hours post-collection) to ensure maximum blood cell viability and minimum perturbations to the cells.

METHODS

QD Synthesis

Cadmium selenide QDs were synthesized in a coordinating solvent following previously published procedures (*Journal Of The American Chemical Society* 2002, *124*, 2049, which is incorporated herein by reference for the corresponding discussion). After purification via precipitations from methanol, the QDs were resuspended in a mixture of ODE and ODA, and then capped with a shell of CdS (2 monolayers) and then ZnS (2 monolayers) at 230°C under argon, using organometallic precursors (*Journal of Physical Chemistry B* 2004, *108*, 18826, *Journal Of The American Chemical Society* 2005, *127*, 7480 and, *Journal of the American Chemical Society* 2003, *125*, 12567, each of which is incorporated herein by reference for the corresponding discussion). These ODA-passivated QDs were stored as a crude mixture at 4°C and purified using repeated extractions in hexane/methanol, followed by precipitations with acetone prior to use. After drying, the QDs were resuspended in THF. QDs were resuspended in THF immediately prior to addition to the reaction mixture.

MNP Synthesis

Fe_3O_4 MNPs were synthesized in oleic acid coordinating solvent following a procedure developed by Sun (*Journal of the American Chemical Society* 2004, *126*, 273, which is incorporated herein by reference for the corresponding discussion). After synthesis, the particles were suspended in hexane. From this hexane solution, the particles were precipitated using methanol and dried prior to use.

Polymers

Typically, polymers were aliquoted as necessary and resuspended in THF or other suitable solvents. Sonication for approximately 30 minutes was used to create a clear solution.

Dialysis Procedure

Nanoparticles and polymer were dissolved in THF, mixed, and then dialyzed repeatedly against deionized water using a low molecular weight cutoff membrane (2000 MW). The dialysis procedure was allowed to proceed over 8-12 hours, with 3-4 changes of buffer. Volumes used were 2-4 mL of polymer-nanoparticle solution dialyzed against 1-2 liters of water. Polymer concentrations ranged between 5 and 25 mg/mL, while starting nanoparticle concentrations ranged from 1-100 nM. For dual modality probes, MNPs and QDs were mixed in varying ratios prior to addition to the polymer solution.

Ultracentrifugation

Initial studies showed that several round of centrifugation and ultracentrifugation could be used to separate the multinanoparticle micelles from excess polymers and ligands. Typically, immediately following dialysis, the resulting solution was centrifuged at 7000 rcf for 20 minutes. This first supernatant was collected and ultracentrifuged at 150,000 rcf for 1 hr. The resulting second supernatant, which usually contained a cloudy mixture of polymer and excess ligands at the top was discarded, and the pellet, which contained single nanoparticles and micelles was re-suspended and subjected to another round of centrifugation at 7000 rcf. This procedure was repeated up to 5 times, until no polymer was visible following ultracentrifugation and the nanoparticles pellet easily resuspended in buffer.

Liquid Chromatography

For large scale separation and purification using liquid chromatography, we used an AKTA Primeplus machine (GE Healthcare). Two different columns were used: Sephacryl 500HR column (bed volume = 45 mL) and Superose 6 (bed volume = 20mL).

Fractions were collected using the autofractionater, and corresponded to desired UV absorption peaks. Typical sample volumes were approximately 1-5 mL.

Fluorescent Microscopy

Nanoparticle loaded micelles were typically spread on a L-polylysine coated coverslip and excited with a mercury arc lamp on a conventional inverted microscope. Alternatively, a single drop of the micelle solution can be placed on a coverslip and allowed to evaporate prior to imaging. Images were captured with a Nikon D100 at 100X magnification. For cell-free experiments, the exposure time was approximately 3 seconds. For granulocyte cellular imaging, higher exposure times were used in order to make sure QD-micelle samples indeed didn't demonstrate any QD fluorescence.

Transmission Electron Microscopy (TEM)

Purified, concentrated samples were dropped on to copper TEM grids with a mesh size of 200 and a formvar polymer coating (Ted Pella). The sample was allowed to rest on the grid for approximately 10 minutes prior to wicking away excess water using filter paper. Phosophotungstenic acid was used to negatively stain the grids by dropping on the grid for approximately 30 seconds prior to being wicked away. The samples were then imaged using a Hitachi H7500 TEM.

Dynamic Light Scattering

Dynamic light scattering (DLS) data was typically obtained on a Brookhaven Instruments 90 plus particle analyzer. The experiment was carried out for 3 runs of 2 minutes each, and analyzed using the "number" (first-order) Multimodal Size Distribution.

Spectroscopy

Spectroscopic measurements were obtained using a Jobin Yvon Fluoromax-2. Scans were run from 490 nm to 680 nm with excitation at 475nm.

MRI Scanner

A Phillips MRI scanner operating at 1.5 Tesla was used to obtain ghost images of micelles in 2.5 mL Eppendorf tubes. Scans of both T1 and T2 relaxivity were taken and data was analyzed using standard techniques.

ICP Spectroscopy

After characterization of purified samples using the MRI Scanner, 3 mL of sample were degraded by adding 1 mL of piranha solution. The mixture was evaporated over night in a desiccator, and sent to University of Georgia chemical analysis lab for ICP spectroscopy. There, the samples were run on a Thermo Jarrell-Ash 965 Inductively Coupled Argon Plasma spectrometer.

RESULTS AND DISCUSSION

Our optimized encapsulation and purification procedure was successful in producing single and multinanoparticle micellar probes as demonstrated by the TEM and DLS data presented in Fig. 2-2. These data show that the nanoparticle size and composition can be varied by adjusting the starting ratio of QDs to amphiphilic polymer. The data also demonstrate that at very high polymer concentrations, samples tend to be more monodisperse. Control of the size and encapsulation of nanoparticles was obtained by adjusting the molar feeding ratio of amphiphilic polymer: nanoparticle. For example, a ratio of 100 mol polymer: 1 mol nanoparticle produced multinanoparticle micelles with an average diameter of 30 nm. By increasing the feeding ration to 500 mol polymer: 1 mol nanoparticle, we were able to produce singly encapsulated nanoparticles with an average diameter of 13 nm. However, at feeding ratios below 100:1, uncontrollable aggregation occurred, and there were no recoverable micellar probes.

It is interesting to note that increasing the polymer:nanoparticle feeding ratio also increased shell thickness of the polymer coating. The thick PEO is thought to reduce adsorption by blood proteins and uptake by immune cells, and is in contrast to the typical "crew cut" polymers with short hydrophilic chains that have been used to create nanoparticle micelles in the past (*Nano Letters* 2005, *5*, 1987, *Langmuir* 2007, *23*, 2198 and, *Journal Of The American Chemical Society* 2005, *127*, 10063, each of which is

incorporated herein by reference for the corresponding discussion). This range of shell thickness is due to higher density polymer packing in the single nanoparticle case as opposed to the multinanoparticle micelles. Studies of the interactions between nanoparticles and other amphiphilic block copolymers have shown similar results (unpublished data). This observation also offers an explanation as to the uncontrollable aggregation that occurs at low polymer: nanoparticle feeding ratios: the polymer is sterically unable to stabilize large numbers of nanoparticles because of reduced polymer-polymer interactions at large micelle sizes. This subsequently causes the assembly process to fail, and rapid nanoparticle-nanoparticle clustering occurs in an attempt to reduce the surface contact area with water.

In general, the size distribution by DLS shows a normal curve with a tail towards larger micelle sizes. There is also a lower limit for micelle size, that of the pure-polymer micelles, 11nm. Since the encapsulation process is fundamentally stochastic, there are always some singly encapsulated QDs produced along with large aggregates (Fig. 2-4). This has an important implication for multimodal nanoparticle based probes: it is nearly impossible to generate completely uniform distributions of two different types of nanoparticles using this system. This same phenomenon has been observed by Taton and coworkers (*Langmuir* 2007, *23*, which is incorporated herein by reference for the corresponding discussion). While this restricts certain applications, such as single-molecule multiplexed detection, it does not hinder end-use goals such as in vivo imaging. Further, the problem can be eliminated entirely by creating single-color micellar probes targeted against a variety of proteins. For example, a yellow QD-micelle probe could be targeted against protein A while red QD-micelles could be targeted against protein B. We have previously published results demonstrating the capability to detect multiple QD colors in a single animal with one imaging procedure (*Nature Biotechnology* 2004, *22*, 969, which is incorporated herein by reference for the corresponding discussion).

As shown in Fig. 1-3, the dialysis-based encapsulation procedure preserved many of the spectral properties of hydrophobic QDs, in particular their narrow spectral width, absorption spectra, and emission peak. Fluorescent imaging and other work in our lab demonstrated that the QD-micelles were highly resistant to photobleaching as with other QD coatings (*Physical Chemistry Chemical Physics* 2006, *8*, 3895, which is incorporated

herein by reference for the corresponding discussion). In addition, it is possible to detect QD blinking both in the single-nanoparticle micelle and in the multinanoparticle micelles. However, the blinking is greatly reduced in the multinanoparticle case. This suggests this micelle encapsulation system may also have use for the study of QD-blinking, a phenomenon which is poorly understood (*New Journal Of Physics* 2005, *7*, *Proceedings Of The National Academy Of Sciences Of The United States Of America* 2005, *102*, 14284, *Physical Review B* 2005, *72*, and *Journal Of Chemical Physics* 2000, *112*, 3117, which is incorporated herein by reference for the corresponding discussion). The slight haze in Fig. 1-3(A) is due to micelle based probes outside of the microscope focal plane. This non-uniform coverslip coating is due to the poly-L-lysine used to assist in micelle immobilization for rapid image taking. Images can be obtained without this coating, but the process is complex, and often times, the total evaporation of water can cause micelle aggregation due to the surface tension of pure water on the glass coverslip.

There was a loss in quantum yield from 75% to 30% (on average), as measured by comparison with Atto dye 610. We attribute this loss in quantum yield to ligand exchange between the THF solvent and octadecylamine on the QD surface, as evidenced by a total loss in fluorescence after leaving solutions of QDs in THF overnight, and the fact that after exchange of THF for water, no further loss in quantum yield was observed. Further, attempts to perform the entire encapsulation procedure in an oxygen-free environment indicated little or no difference between the open air case and the oxygen free-case, demonstrating that the loss in fluorescence is not due to oxidation of the QD surface. Others have observed a similar phenomenon, but were unable to determine the cause (*Langmuir* 2007, *23*, 2198, which is incorporated herein by reference for the corresponding discussion).

It is important to note that high quantum yields are necessary for QD-micelle based probes to be useful for biological imaging purposes. Several reports have demonstrated that for truly useful biological labels, the lower bound of fluorescence quantum yield should be no lower than 10%, (*European Radiology* 2003, *13*, 195 and *Science* 1998, *281*, 2013, each of which is incorporated herein by reference for the corresponding discussion), which our encapsulation procedure readily provides. It is tempting to suggest changes to the solvent system to enhance quantum yield. However,

we conducted extensive studies comparing various polymers and solvents that show only a few combinations of polymer-solvent pairs can create nanoparticle-micelles through dialysis. Specifically, the polymers must form strong hydrophobic interactions with the QD-surface ligands and the solvents used must solubilize all reactants well, including the nanoparticles and polymers. Further, the solvent system must be soluble in water to achieve facile solvent replacement and suspension in biologically useful buffers. For these reasons, THF and the PMMA-PEO polymer are well suited for producing the micellar probes described here.

The probes' size and morphology are very similar to the QD-only micelles presented earlier. This is expected, as the size and surface coating of the Fe_3O_4 nanoparticles are nearly identical to that of QDs. We also attempted to create T1-weighted optomagnetic probes using a hydrophobic gadolinium chelate (Resolve-AI), QDs, and the dialysis procedure described in the methods section (data not shown). These efforts met with mixed results. The PMMA-PEO clearly solubilized the chelate, as samples containing no polymer precipitated upon dialysis while polymer containing samples formed clear micelle solutions, and displayed strong fluorescence in the case with nanoparticle-only samples. Strong T1 signal was observed immediately after the encapsulation through dialysis. However, after purification, the T1 signal was all but lost, indicating that the small molecule chelate either leached out of the nanoparticle containing micelles or was only encapsulated in excess polymer micelles.

The strong optical and magnetic resonance imaging properties created by this approach are an important step towards realization of true clinical dual modality imaging, where a surgeon could visually identify small tumors or lesions prior to surgery with MRI, and then use the fluorescent probe capability to completely remove the diseased tissue during operation (*Cancer Research* 2003, *63*, 8122, which is incorporated herein by reference for the corresponding discussion).

CONCLUSIONS

In conclusion, we have demonstrated a new approach for the development of bioimaging probes using amphiphilic block copolymers and high quality inorganic nanoparticles. The approach detailed here has the following advantages: 1) the use of

high quality QDs improves probe brightness 8x over previously reported attempts 2) the use of Fe_3O_4 MNPs as opposed to Fe_2O_3 allows strong T2-weighted MRI contrast while using lower MNP:QD ratios 3) the PEO coating on the surface of the micelles endows remarkable chemical and biological stability, 4) the use of dialysis to assemble the probes and FPLC to purify the reactant mixture allows production of several moralities at milligram quantities, and 5) no cross-linking is necessary to create stable probes. Currently, we are developing methods for incorporating functional sites on the micelle surface to allow attachment to biological molecules using end-modified block copolymers.

Example 3

As shown in Fig. 3-1, the polymer used is slightly structurally different from PEO-PMMA. It is interesting to note that while conducting our survey of various potential block copolymers, a tButMA-PEO conjugate was used but the polymer caused precipitation in its pure form. However, when used as a doping reagent in the dialysis procedure, the polymer can be incorporated into the micelles. The hypothesis behind this approach is that the micellazation process of soluble PMMA-PEO can trap a certain amount of tButMA-PEO and help suspend it. The fluorescamine data in Fig. 3-2(B) supports this hypothesis, as increasing the loading ratio of tButMA-PEO resulted in increased free amine content in purified micelles. Two controls in Fig. 3-2(A) show the fluorescamine signal for pure water and the tButMA-PEO in water. tButMA-PEO has a very low solubility in water, and these samples were created by adding 10 mg of the polymer to 1 mL of water and vigorously stirring and sonicating the sample. Even after the vigorous mechanical treatment, the polymer still largely remained as a solid. Thus, we were surprised to find any fluorescamine signal in the pure sample. However, given the fact that there are large PEO chains on the polymer, it stands to reason that a certain percentage would be soluble in water. The PEO chains themselves have some polydispersity, so it is likely that the soluble amphiphilic polymers are those with the largest PEO chains. Controls on polymers that were still protected showed no fluorescent signal, which further indicates that the fluorescamine signal was indeed due to the free amine on the polymer and not to any other reason. It is also interesting to note that the

absolute fluorescamine signal for these polymer-only samples was significantly stronger than the doped micelle samples. This difference is likely due to a combination scattering and the presence of other polymers that can sterically interfere with the fluorescamine reaction.

The amount incorporated is a small percentage of the total feeding ratio, as there is a significant amount of suspended tButMA-PEO that is removed during the filtration of the micelle product. However, the flourescamine data in Fig. 3-2 show that there is still a substantial amount of polymer available for reaction, and this amount can be tuned by adjusting the feeding ratios of the functionalized polymer to the unfunctionalized polymer. It is important to note that because our micelle probes are extremely stable in harsh chemical conditions, the deprotection step can be carried out at pHs below 3.

Conjugation to Folic Acid

Having created a functionalized micelle, we attempted to attach folic acid residues to the deprotected amine groups on the micellar shell. To accomplish this, we added deprotected multinanoparticle micelles, NHS-acitivated folic acid, and EDC in a slightly acidic buffer. We then separated the reactants using FPLC. The results of the first attempt are shown in Fig. 3-3. Fig. 3-3(A) shows differences in elution time between conjugated and non-conjugated micelles. The conjugated peak (pink) exhibits an extended elution time as compared to our traditional micellar probes (pink), with very little increase in peak width. However, because the samples were so dilute, we were unable to recover this peak for further testing and verification. For reference, in Fig, 3-4 we show the entire chromatogram with no scaling for the micelle folic acid reaction mixture. The large peak is indicative of free, unreacted folic acid.

There are several factors that can be modified in the future to improve conjugation efficiency. First, the amine content of the micellar probes needs to be optimized. In this instance, it should be increased to as high a content as possible without disrupting the dialysis process. Secondly, the pH of the reaction should be modulated to determine the optimal conditions for conjugation. Folic acid has poor solubility in acidic conditions, so running the EDC reaction in more basic conditions should improve yield. Finally, the non-functionalized PEO chains could interfere with the reaction by creating

steric interference between the reacting Folic acid and deprotected amine groups. As such, rather than simply keep a protecting group on the tail of the PEO domain, one could envision an alternate approach where targeting ligands were attached to the polymer prior to micellization. We did not attempt this approach based on our experiences with the micellization process. The process is very sensitive to molecular structure and even slightly different hydrophobic block structures can cause uncontrollable aggregation. A pertinent example is the fact that the tButMA-PEO-NH2 polymer will not form micellar probes when it is in large excess. Rather, it must be doped as described to ensure solubilization and formation of stable probes. Nonetheless, with a small molecule such as folic acid, it may be possible to dope the micelles in a similar fashion to that described in this chapter.

Two major conclusions can be drawn from the data presented in this Example. First, amine coupling two polymers end to end can work as a synthetic strategy, but it is extremely low yield, and unlikely to produce polymers in sufficient quantity or quality to be useful for further derivitization. Secondly, it is possible and relatively easy to dope micelles with similar, but not structurally identical amphiphilic polymers. These polymers can have protected end groups that can then be deprotected to yield active functional groups on the micelle surface.

Example 4

This Example demonstrates fluorescent imaging of PMMA-PEO micelles compared to polyacrylic acid micelles after incubation in human plasma for 24 hours. The PMMA-PEO micelles show very little aggregation while the polyacrylic acid micelles are significantly aggregated. This data is shows charged polymers are quickly aggregated in biological buffers

To demonstrate the superior biocompatibility of our micellar probes as compared to other strategies, we performed a variety of tests in harsh chemical and biological conditions. As expected from the initial design, micelles coated with PEO performed far better than polyacrylic acid based coatings in terms of reduced opsonization, internalization, and aggregation. Fig. 4-1 shows the results of incubating micelles and polyacrylic acid coated QDs with granulocytes in the presence of human plasma for 24 hr

at 37^0C. Granulocytes are the scavengers of the immune system, and remove foreign bacteria and toxic substances through phagocytosis. The stages of phagocytosis include opsonization, uptake, release to the granulocyte cytoplasm, and finally, break down by lytic enzymes in the granulocyte. Opsonization and degradation are the two most important processes nanoparticle surface coatings can affect. Opsonization is the tagging of foreign bodies by blood born proteins, which then trigger uptake by granulocytes. Because our probes are highly resistant to protein binding, they reduce the opsonization process and increase circulation lifetimes. Secondly, during the degradation process, granulocytes use the myeloperoxidase enzyme. This enzyme catalyzes a reaction with hydrogen peroxide which breaks down the foreign substance, and may cause the release of toxic Cd ions in the case of QDs (*Nano Letters* 2005, *5*, 331, which is incorporated herein by reference for the corresponding discussion). As we have demonstrated, not only are our micellar probes stable against opsonization, but they remain stable in hydrogen peroxide environments, which are even more stringent that what is found in a granulocyte (*Physical Chemistry Chemical Physics* 2006, *8*, 3895, which is incorporated herein by reference for the corresponding discussion).

The polyacrylic acid coated QDs in Fig. 4-2(A) are aggregated and internalized by the granulocytes, while in Fig. 4-2(B), the micelles have been able to avoid entrapment due to the thick PEO coating on the micelle surface. This result is in good agreement with others in our lab which show that neutral coatings show reduced aggregation, uptake by immune cells, and non-specific binding (Sathe and Nie, unpublished data) as compared to positively or negatively charged coatings. We also incubated pure human plasma and each nanoparticle coating at 37^0C for 24vhours in the absence of cells, and imaged the purified samples on coverslips. The results show significant aggregation in the case of polyacrylic acid coating while the PEO micelles still spread uniformly. In sum, the studies of our micellar coating as compared to other coatings have shown significant advantages in terms of chemical stability and biocompatibility.

Having verified that the micelles are not significantly aggregated by blood plasma, we wanted to determine whether or not there were any adsorbed proteins that could create a micelle-protein complex. This type of non-covalent interaction has been

observed by others for all nanoparticle coatings. To determine this, we decided to use agarose gel-electrophoresis. The choice of this technique would allow us to easily visualize differences in electromobility, where as our FPLC and imaging assays only allowed us to assess hydrodynamic radius. To accomplish this, we incubated several nanoparticle samples with human plasma for 24 hours, and then loaded them into consecutive lanes in an agarose gel. The results in Fig. 4-3 highlight several interesting phenomena that were observed. First, the PMMA-PEO micelles do not leave the well appreciably with no plasma incubation while polyacrylic acid coated nanoparticles show significant mobility, due to their high surface charge. It should be noted that these behaviors are reversed after incubation with plasma for 24 hours. In the case of the polyacrylic acid coated QDs, the lack of mobility must be due to the aggregation of these QDs, as supported by the results from the FPLC and fluorescent imaging data. However, in the case of the micellar probes, the change in behavior must be solely due to non-covalent interactions with the plasma. These noncovalent interactions then result in charged micelle-protein complexes that can migrate through the gel. These conclusions are supported by several observations. The FPLC and imaging data demonstrate that the micelles exhibit no dramatic increase in aggregation or hydrodynamic radius, which is supported by the fact that the micelles are able to migrate after incubation with plasma, and are not trapped inside the wells, as is the case with polyacrylic acid QDs. Further, the fact that micelles do not migrate in gels with no plasma indicate they must have gained charge to gain electrophoretic mobility.

If the probes do not form noncovalent micelle-protein complexes, there is the possibility that the micelles are forced to move due to the overall charge of the plasma, much like a traditional loading buffer. Another possibility is that the proteins interfere with the micelles, and "push" them along through the gel although they are not truly bound together. This would make sense as many the proteins in plasma are have similar elution time to micelles in FPLC. Whatever the case, the interaction clearly does not cause the degree of aggregation seen with polyacrylic acid coated micelles, or any adverse effects to the micelles' emission properties.

After examining the interaction of PMMA-PEO micelles and polyacrylic acid in the presence of plasma, we turned our attention to whole blood assays with phagocytic

white blood cells present. Specifically, we chose to investigate the interaction with isolated granulocytes. Granulocytes are the scavengers of the immune system, and remove foreign bacteria and toxic substances through phagocytosis. The stages of phagocytosis include opsonization, uptake, release to the granulocyte cytoplasm, and finally, break down by lytic enzymes in the granulocyte. Opsonization and degradation are the two most important processes our design accounts for. Opsonization is the tagging of foreign bodies by blood born proteins, which then trigger uptake by granulocytes. Because our probes are highly resistant to protein binding, they reduce the opsonization process and increase circulation lifetimes. Secondly, during the degradation process, granulocytes use the myeloperoxidase enzyme. This enzyme catalyzes a reaction with hydrogen peroxide which breaks down the foreign substance. As we have demonstrated, not only are our micellar probes stable against opsonization, but they remain stable in hydrogen peroxide environments, which are even more stringent than what is found in a granulocyte.

Conclusions

The results presented in this Example demonstrate some of the advantages of our PEGylated micellar multi-nanoparticle coating as opposed to carboxylated coatings used by others. It is not surprising that PEGylation greatly reduces nospecific adsorption of plasma proteins and uptake by granulocytes. However, the degree to which these micellar probes are stable both in stringent biological and chemical conditions is surprising. The wide range of chemical, photostable, and other conditions explored here show the wide diversity of these probes, and point towards *in vivo* utility.

It should be noted that ratios, concentrations, amounts, and other numerical data may be expressed herein in a range format. It is to be understood that such a range format is used for convenience and brevity, and thus, should be interpreted in a flexible manner to include not only the numerical values explicitly recited as the limits of the range, but also to include all the individual numerical values or sub-ranges encompassed within that range as if each numerical value and sub-range is explicitly recited. To illustrate, a concentration range of "about 0.1% to about 5%" should be interpreted to

include not only the explicitly recited concentration of about 0.1 wt% to about 5 wt%, but also include individual concentrations (*e.g.*, 1%, 2%, 3%, and 4%) and the sub-ranges (*e.g.*, 0.5%, 1.1%, 2.2%, 3.3%, and 4.4%) within the indicated range. The term "about" can include ±1%, ±2%, ±3%, ±4%, ±5%, ±6%, ±7%, ±8%, ±9%, or ±10%, or more of the numerical value(s) being modified. In addition, the phrase "about 'x' to 'y'" includes "about 'x' to about 'y'".

It should be emphasized that the above-described embodiments of the present disclosure are merely possible examples of implementations, and are merely set forth for a clear understanding of the principles of this disclosure. Many variations and modifications may be made to the above-described embodiment(s) of the disclosure without departing substantially from the spirit and principles of the disclosure. All such modifications and variations are intended to be included herein within the scope of this disclosure and protected by the following claims.

CLAIMS

Therefore the following is claimed:

1. A micellar structure, comprising:

a plurality of nanoparticles and amphiphilic copolymers, wherein the amphiphilic copolymers include hydrophobic blocks and hydrophilic blocks, wherein the hydrophilic blocks of the amphiphilic copolymers form an outer shell around the plurality of nanoparticles, wherein the hydrophobic blocks of the amphiphilic copolymers interact with the nanoparticles within the outer shell of the micellar structure, and wherein the micellar structure is about 10 to 100 nm in diameter.

2. The micellar structure of claim 1, wherein the plurality of nanoparticles are selected from: magnetic nanoparticles, semiconductor nanoparticles, metal nanoparticles, metal oxide nanoparticles, metalloid and metalloid oxide nanoparticles, lanthanide metal nanoparticles, or combinations thereof.

3. The micellar structure of claim 1, wherein the plurality of nanoparticles includes quantum dots.

4. The micellar structure of claim 1, wherein the amphiphilic copolymer is a polymethylmethacrylate-PEG block copolymer.

5. The micellar structure of claim 1, wherein the nanoparticles are about 50% to 99.9% weight percent of the micellar structure and wherein the amphiphilic copolymer is about 0.1% to 5% weight percent of the micellar structure.

6. The micellar structure of claim 1, wherein the plurality of nanoparticles includes quantum dots, and wherein the amphiphilic copolymer is a polymethylmethacrylate-PEG block copolymer.

7. The micellar structure of claim 6, wherein the nanoparticles include at least two types of quantum dots, where each type of quantum dot emits at a different wavelength.

8. The micellar structure of claim 6, wherein each of the nanoparticles have a tri-octylphosphine oxide capping ligand disposed on the surface of the nanoparticle that interacts with the polymethylmethacrylate-PEG block copolymer.

9. The micellar structure of claim 1, wherein amphiphilic copolymers are selected from: amphiphilic block copolymers, amphiphilic random copolymers, amphiphilic alternating copolymers, amphiphilic periodic copolymers, or combinations thereof

10. The micellar structure of claim 1, further comprising an agent attached to the micellar structure, wherein the agent is selected from a therapeutic agent or biological agent.

11. A method of making micellar structures, comprising:
providing a nanoparticle and an amphiphilic copolymer;
mixing the nanoparticle and the amphiphilic copolymer in a solvent;
replacing the solvent with water; and
forming the micellar structures.

12. The method of claim 11, wherein the solvent is selected from: tetrahydrofuran, methanol, isopropyl alcohol, ethanol, 1,4 dioxane, dimethyl sulfoxide, n,n-dimethlyformamide, acetnonitrile, acetone, or combinations thereof.

13. The method of claim 11, wherein the ratio of the nanoparticle to amphiphilic copolymer is about 1:100.

14. The method of claim 11, wherein replacing the solvent with water includes using a system selected from a dialysis system or an ultrafiltration system.

15. The method of claim 11, wherein replacing the solvent with water includes introducing the solvent including the nanoparticle and the amphiphilic copolymer to a dialysis system, wherein the dialysis system includes a water, wherein the dialysis system includes a dialysis membrane that separates the water and the solvent including the nanoparticle and the amphiphilic copolymer, wherein the water replaces the solvent so that the micellar structures are formed and are in the water solution.

16. The method of claim 15, further comprising:

separating the micellar structures from the residual amphiphilic copolymer in the water solution.

17. The method of claim 15, further comprising:

separating the micellar structures from aggregation in the water solution

18. The method of claim 15, wherein the nanoparticles are quantum dots, and wherein the amphiphilic copolymer is a polymethylmethacrylate-PEG block copolymer.

19. The method of claim 18, wherein the solvent is tetrahydrofuran.

20. The method of claim 18, wherein each of the nanoparticles have a tri-octylphosphine oxide capping ligand disposed on the surface of the nanoparticle that interacts with the polymethylmethacrylate-PEG block copolymer.

21. The method of claim 15, wherein the nanoparticles are selected from: magnetic nanoparticles, semiconductor nanoparticles, metal nanoparticles, metal oxide nanoparticles, metalloid and metalloid oxide nanoparticles, lanthanide metal nanoparticles, or combinations thereof.

22. A method of imaging a host, comprising:

providing the micellar structure of claim 1;

administering the micellar structure to the host; and

imaging the host.

23. The method of claim 22, wherein the micellar structure includes a biomolecule having an affinity for a target.

24. The method of claim 22, wherein imaging the host includes:

determining the location of the micellar structure, wherein the location of the micellar structure corresponds to the location of the target.

25. The method of claim 24, wherein the target is selected from: a disease, a condition, a precancerous cell, cancer, tumor, or physical abnormality.

26. The method of claim 22, wherein the plurality of nanoparticles includes quantum dots, and wherein the amphiphilic copolymer is a polymethylmethacrylate-PEG block copolymer.

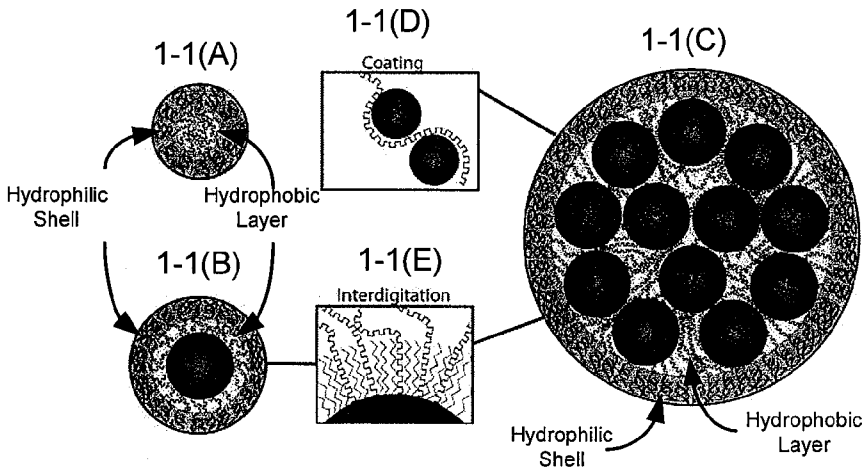
1-1(A)
1-1(D)
Coating
1-1(C)
Hydrophilic Shell
Hydrophobic Layer
1-1(B)
1-1(E)
Interdigitation
Hydrophilic Shell
Hydrophobic Layer

Fig. 1-1

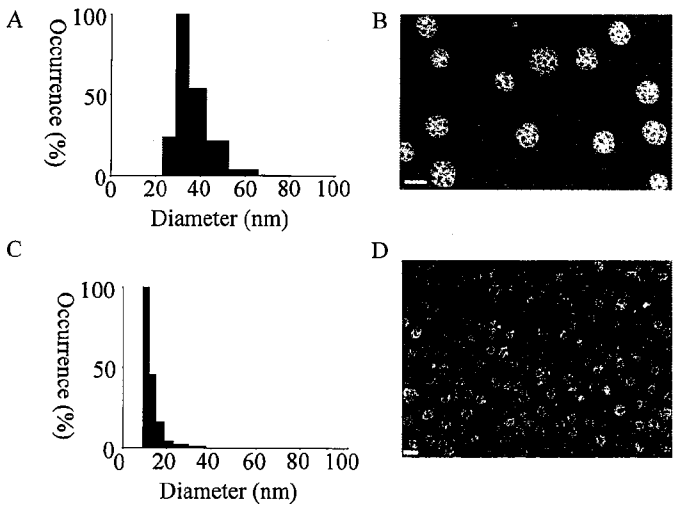
A
100
50
0
Occurrence (%)
0 20 40 60 80 100
Diameter (nm)
B
C
100
50
0
Occurrence (%)
0 20 40 60 80 100
Diameter (nm)
D

Fig. 1-2

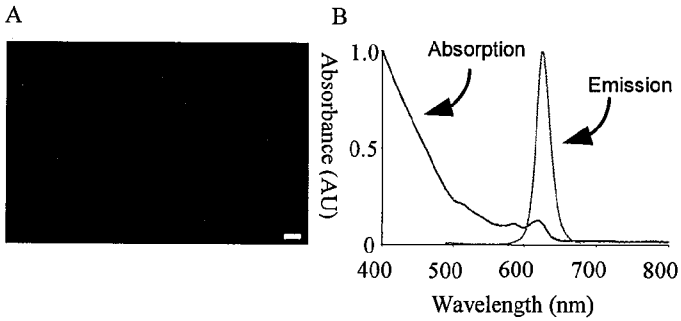
A
B
1.0
0.5
0
Absorbance (AU)
Absorption
Emission
400
500
600
700
800
Wavelength (nm)

Fig. 1-3

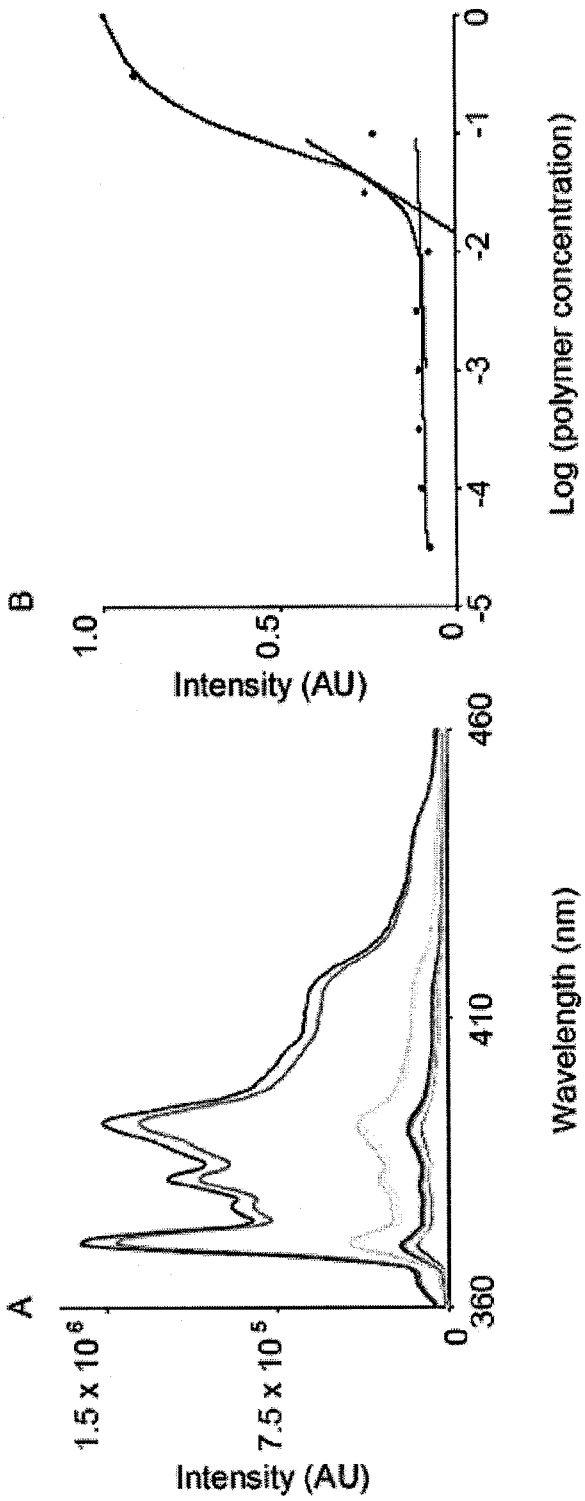
A
1.5 x 10^6
7.5 x 10^5
Intensity (AU)
0
360
410
460
Wavelength (nm)
B
1.0
0.5
0
Intensity (AU)
0
-1
-2
-3
-4
-5
Log (polymer concentration)

Fig. 1-4

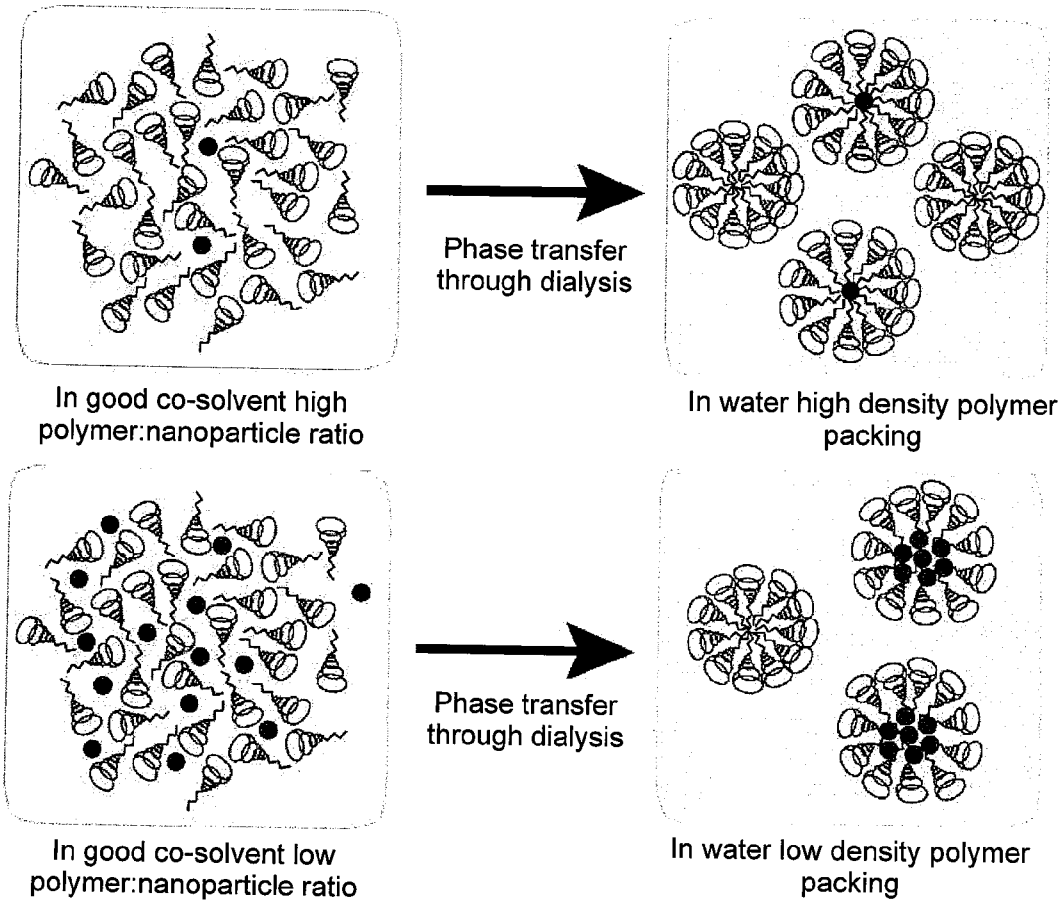

Fig. 2-1(A)(top) and 2-1(B)(bottom)

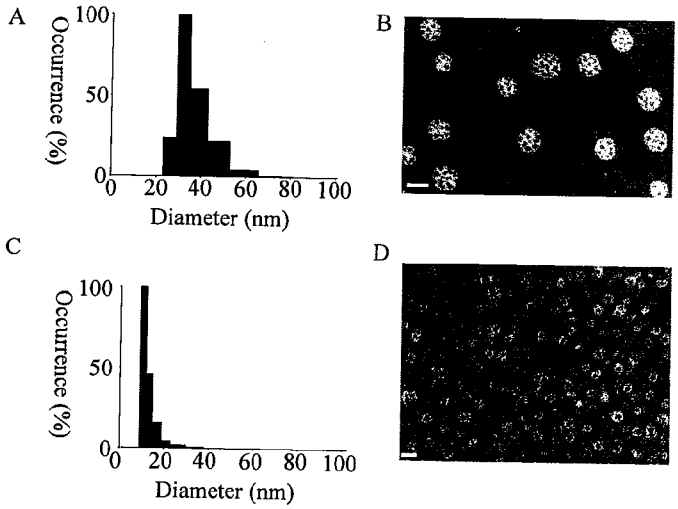

Fig. 2-2

Fig. 2-3

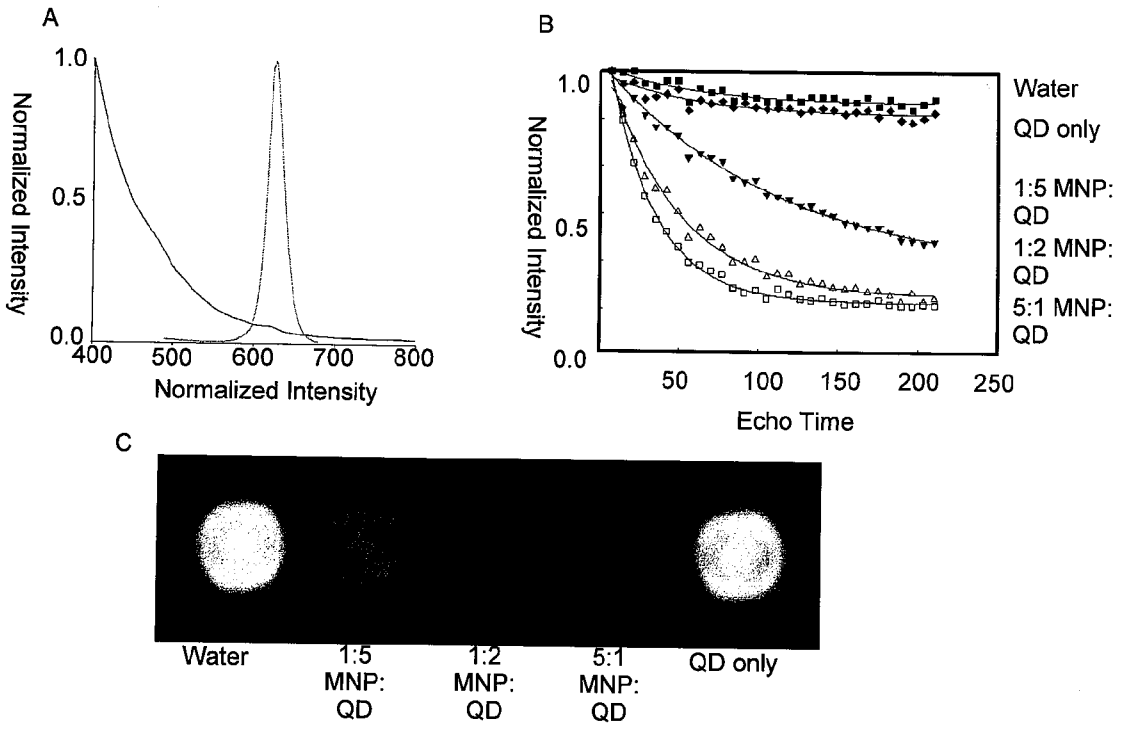
A
1.0
0.5
0.0
Normalized Intensity
400
500
600
700
800
Normalized Intensity
B
1.0
0.5
0.0
Normalized Intensity
50
100
150
200
250
Echo Time
Water
QD only
1:5 MNP: QD
1:2 MNP: QD
5:1 MNP: QD
C
Water
1:5 MNP: QD
1:2 MNP: QD
5:1 MNP: QD
QD only

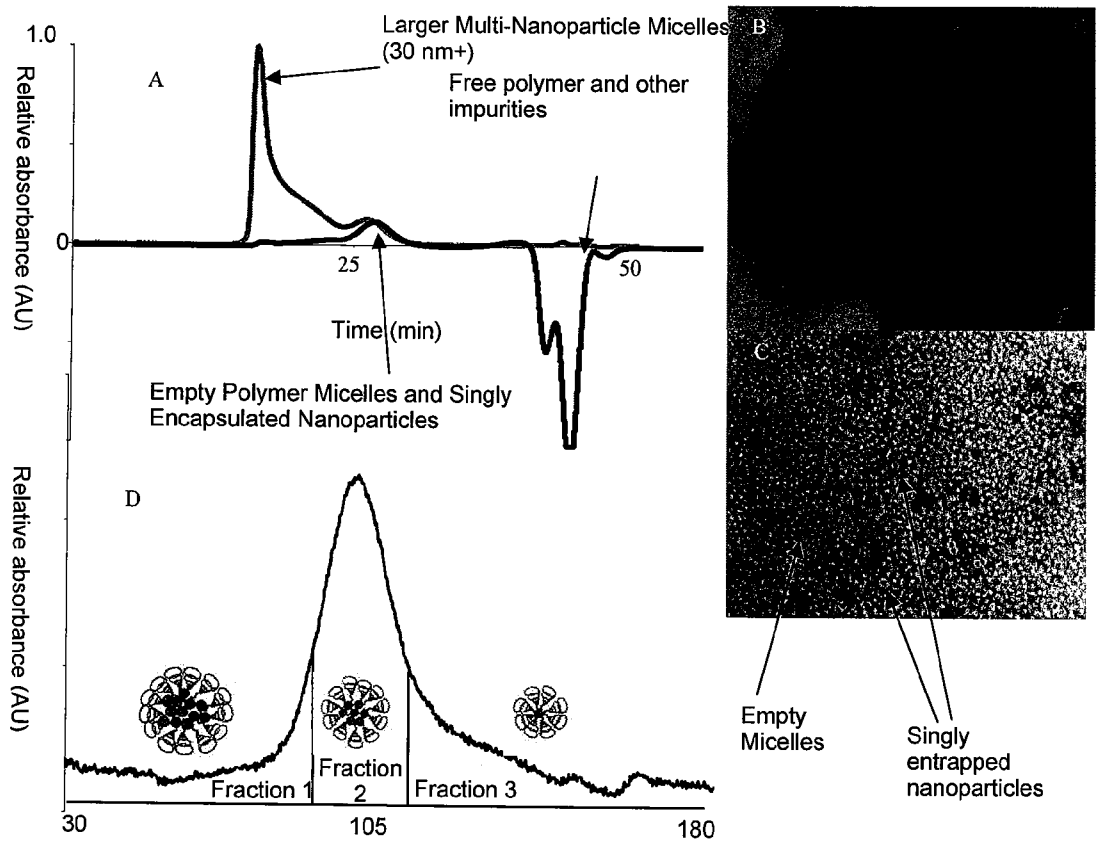
1.0
Relative absorbance (AU)
A
Larger Multi-Nanoparticle Micelles (30 nm+)
Free polymer and other impurities
0
25
50
Time (min)
Empty Polymer Micelles and Singly Encapsulated Nanoparticles
B
C
Empty Micelles
Singly entrapped nanoparticles
D
Relative absorbance (AU)
Fraction 1
Fraction 2
Fraction 3
30
105
180

Fig. 2-4

Boc-NH-PEG-COOH Mw = 10,000
+
PMMA-NH2 Mw = 8,900
=
BocNH-PEO-PMMA Mw =18,900

Materials for Approach I: "Mimicking"

tbutMA - PEO-NH-disilyl

Mw = 3,500 Mw = 13,000

Materials for Approach II: "Doping"

Fig. 3-1

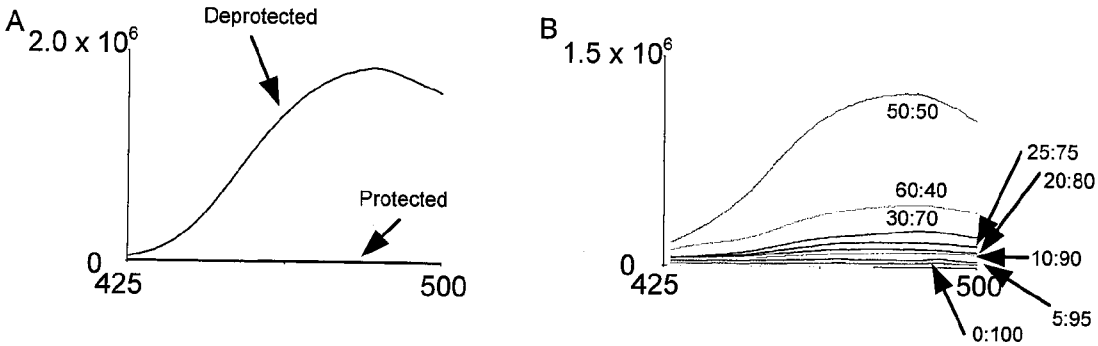

Fig. 3-2

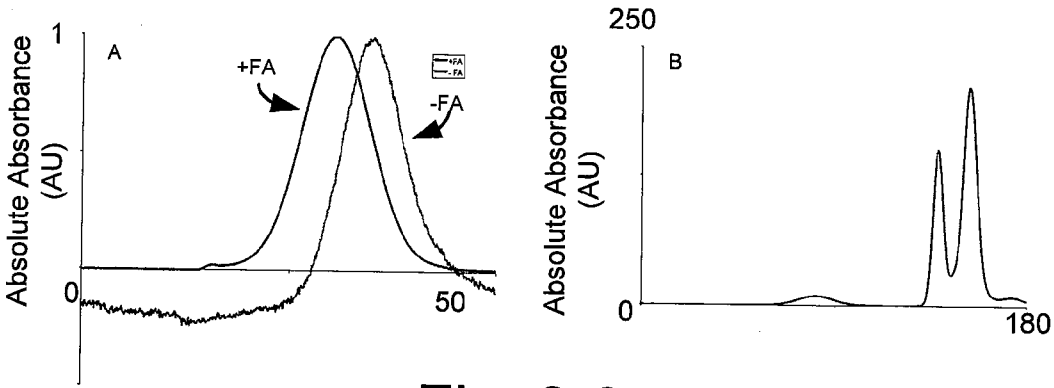

Fig. 3-3

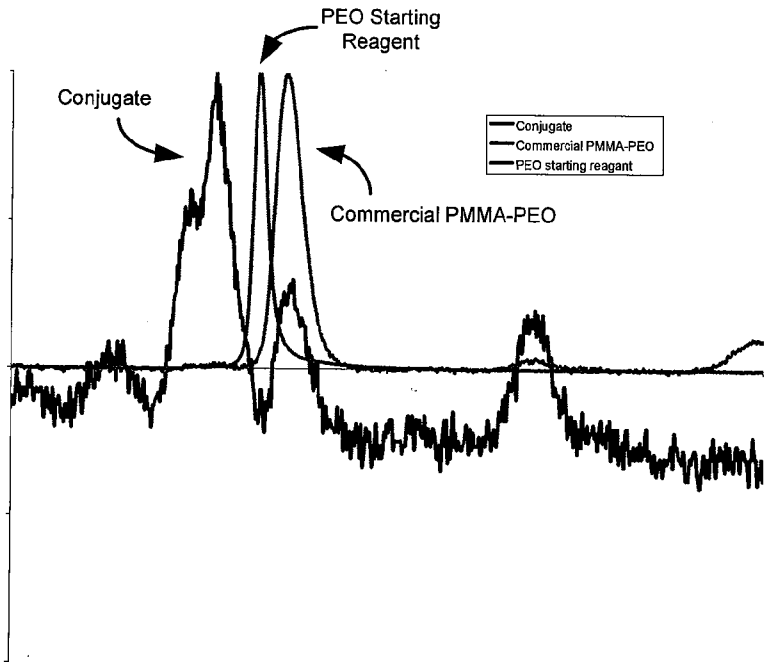
PEO Starting Reagent
Conjugate
Commercial PMMA-PEO
Conjugate
Commercial PMMA-PEO
PEO starting reagant

Fig. 3-4

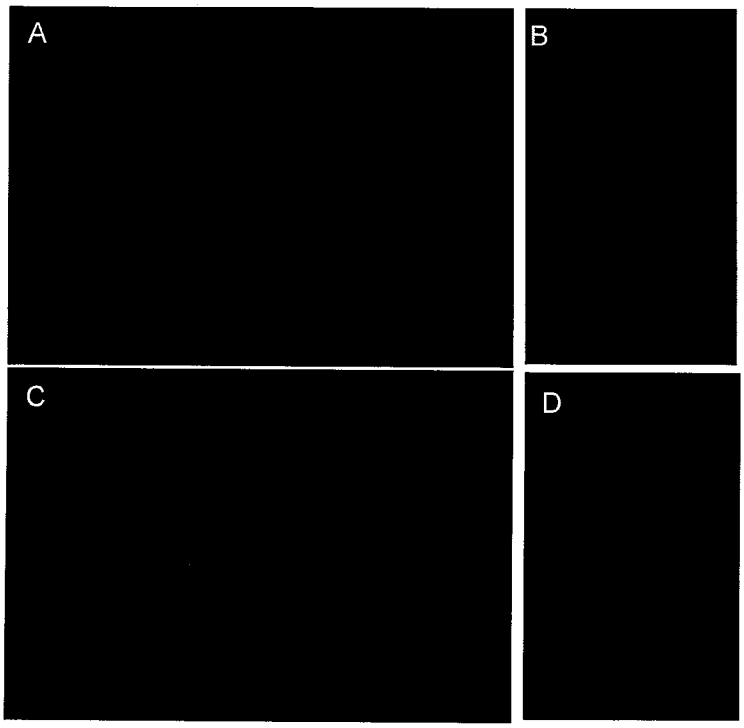

Fig. 4-1

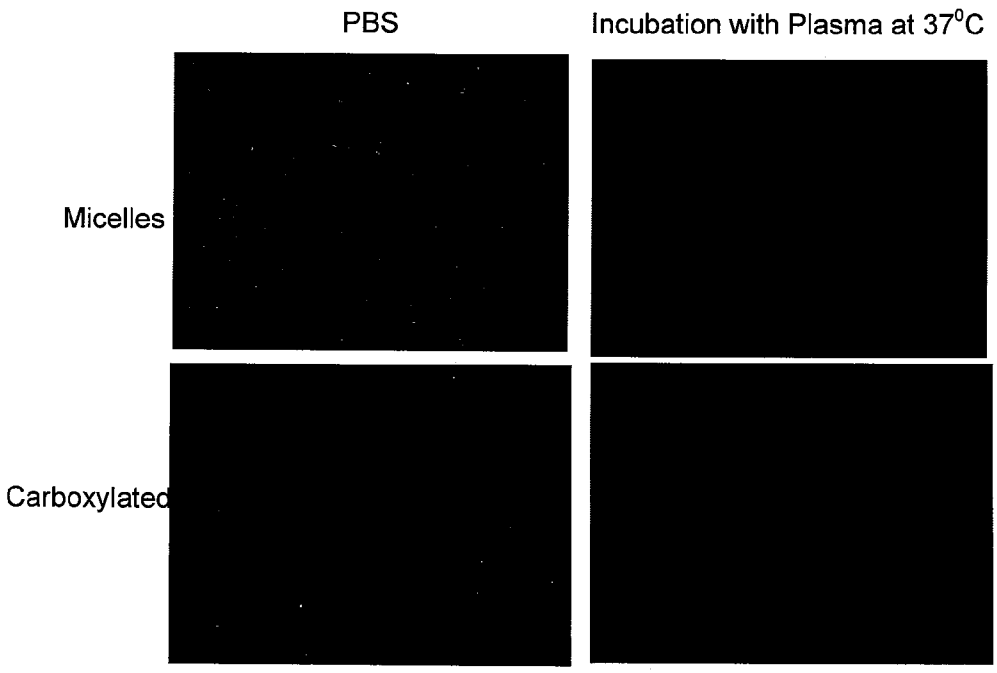

Fig. 4-2

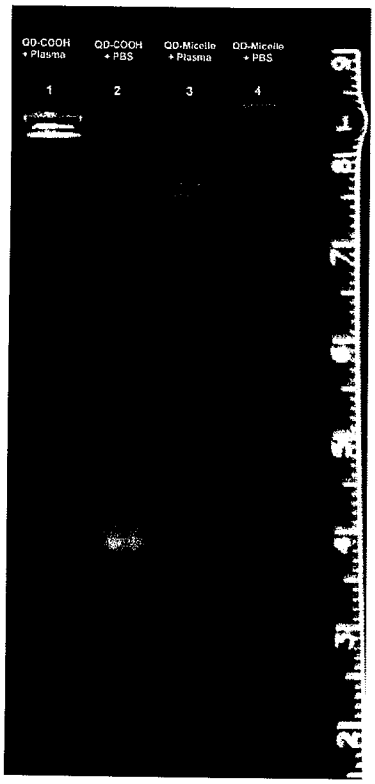
QD-COOH + Plasma
QD-COOH + PBS
QD-Micelle + Plasma
QD-Micelle + PBS
1
2
3
4

Fig. 4-3